UNITED STATES DEPARTMENT OF THE INTERIOR

GEOLOGICAL SURVEY

Geologic applications of thermal-inertia mapping from satellite

by

Kenneth Watson
Susanne Hummer-Miller
Terry W. Offield

Open-File Report 81-1352
1981

1.0 PREFACE

1.1 OBJECTIVES

The principal objective of this study was to investigate applications of HCMM (Heat Capacity Mapping Mission) satellite data in detecting and mapping geologic features for energy-resource and mineral-deposit studies. Other, related objectives involved the development of new techniques and approaches in thermal modeling and image processing.

1.2 SCOPE

The analysis was somewhat restricted by the limited number of sequential day/night image pairs free of major atmospheric/weather problems. For the Powder River Basin, Wyo. area, a single thermal-inertia image was formed using 20 August 1978 data. Four additional nighttime scenes were used to examine geologic formation boundaries and thermal lineaments. The analysis of the Cabeza Prieta, Ariz., area was done using a thermal-inertia image constructed from data acquired April 3 and 4, 1979. No successful U-2 aircraft data acquisition flights were conducted over these two sites so that comparison of different resolution thermal data was only conducted using USGS aircraft data. Despite all these limitations, significant geologic information was derived in this study, and the results suggest the importance of a follow-on thermal satellite experiment for improved mineral and energy resource exploration.

1.3 CONCLUSIONS

Despite limited data, investigations in the Powder River Basin area of eastern Wyoming and adjacent States clearly showed that geologic units as narrow as two or three resolution elements, but of moderate to high thermal-inertia contrast against surroundings, can be discriminated in optimal images. It appears likely that subtle facies differences in sedimentary basin-fill units can be delineated and mapped using satellite thermal-inertia images, especially if sequential images can be obtained during a drying cycle after rain or snow. A few subtle but mappable thermal-inertia anomalies coincide with areas of anomalous helium in soil gas believed to indicate leakage from deep oil and gas concentrations; the presence of thermal-inertia anomalies suggests that gas leakage has produced chemical changes and cementation at the surface. Such changes also are known to be associated with shallow uranium deposits and changes were looked for but not found in the thermal-inertia images; it is thought that the surface changes in this area are too minor and discontinuous to be detected from satellite.

The most consistently practical and important results involve delineation of tectonic framework elements such as lineaments bounding apparent structural blocks. These commonly can be seen even in less-than-optimal data. One pair of major thermal lineaments in the southern Powder River Basin seems to define structures not previously recognized but consistent with, and adding importantly to, an emerging story of basement-block movements and their direct influence on sedimentation, which in part controls the occurrence of large oil and gas resources. One of these lineaments matches up with aeromagnetic map data and appears to reveal a basement discontinuity which underlies the famous

Homestake Mine in the Black Hills and a zone of Tertiary igneous activity. Along with the newly identified lineaments, the thermal images also permit mapping of geomorphic textural domains. The geologic significance of these is not yet understood, but it seems likely that they connote structural and lithologic conditions which affect or control local ground-water regimes.

Similar applications of HCMM data to the Cabeza Prieta, Ariz., area illustrate the potential of using thermal-inertia data for discrimination between extrusive and intrusive rocks and for detecting differences in the mafic content of volcanics. Other results included detection of differences among surficial units - tentatively ascribed to changes in soil-moisture retention, discovery of discrepancies in existing geologic maps, and possible application of the thermal-inertia technique to mapping buried pediments.

Extension from beyond the originally proposed study areas to Yellowstone National Park was made to examine the usefulness of HCMM data in geothermal studies. Although we found that the night-thermal data could not be used with any confidence to distinguish surface hydrothermal features, we did detect additional structural information concerning the outline of the caldera which is the source of the volcanic heat. This reinforces our conclusion that a major utility of these data is in providing information about local-area or regional tectonic framework.

We have also made significant advances in modeling analysis and image-registration techniques. A thermal-inertia mapping algorithm has been developed based on a new method to derive the regional meteorologic parameters solely from the satellite data. An algorithm for determining the sensible-heat flux from ground-station data was also constructed. Simple forms for

four of the atmospheric flux terms were constructed from field measurements made during circumstances when satellite data are likely to be most useful. These forms eliminate the need for extensive continuous ground station data. Also, a method to correct thermal and thermal-inertia data for elevation variations in sky and solar flux was determined. In addition, we have devised a fast topographic adjustment algorithm which can be used in conjunction with digital terrain data to correct the thermal-inertia image for simple topographic slope effects. Finally, a fast image registration technique was developed that proved to be considerably more accurate than the NASA registered products.

Our analysis of the HCMM data has resulted in the recognition of features which suggest the existence of previously unmapped and unknown geologic structures. Their relationship to other geophysical and geochemical data provides important information for a basic resource-exploration strategy. Additionally, substantial progress has been made in modeling and image-processing techniques. This report covers new areas and represents significant advances in the processing and interpretation of thermal satellite data and in the integration of thermal-infrared data in regional geologic exploration.

1.4 RECOMMENDATIONS

From our experience to date, we would recommend that serious consideration be given to a follow-on thermal satellite mission with these general characteristics.

1. The current NEΔT of HCMM seems adequate for most regional studies. Higher thermal resolution does not appear necessary.

2. Some increase in ground resolution (possibly 100-200 m) would be useful; however, there are trade-offs to consider here. The 500-m resolution from HCMM has proven very useful for regional structures - it does not appear promising for detecting alteration.

3. Some increase in the repeat times over a site is desirable. The HCMM data we have seen have often baffled us because of changing meteorologic effects. The increased repeat time would enhance the chances of "stable-clear" conditions and also provide coverage of regions under several meteorological and soil moisture conditions. The repeat time involves the orbit parameter selection; a 5-10 day repeat of coverage would be desirable.

4. The current overflight times of HCMM appear appropriate for geologic analysis. It should also be noted that the daytime maximum represents an optimum time to acquire multispectral thermal measurements as well.

5. Our analysis of HCMM data requires registration of day and night images and subsequent registration to a topographic base. The registered data provided by NASA often contained large registration errors. An essential requirement for analysis of these data is that the clear scene images be registered (day/night images) to a pixel, and to digital terrain data. If this registration accuracy cannot be achieved routinely, it is recommended that registered products <u>not</u> be provided to users.

CONTENTS

ILLUSTRATIONS

Table Page

2.0 INTRODUCTION

The HCMM data which we have examined have provided us with unique geologic information which is both complex to analyze and difficult to explain. In some cases we are astonished to see subtle distinctions of structure and geologic materials that are not found on detailed geologic maps. In other cases we are unable to differentiate widely dissimilar geologic materials or identify features which are clearly described on regional geologic maps or Landsat images. Commonly, geologic features are clearly displayed on a single image or part of an image and not on others. Further complicating the analysis of these data has been the experimental nature of the satellite mission, which has introduced both significant time lags between data acquisition and interpretation, and unique constraints in image registration and data calibration.

This report comprises pieces to a puzzle--a puzzle with tantalizing new information but sufficient gaps to preclude a complete overall assessment. We have examined the geologic implications of the HCMM data in the Powder River Basin of Wyoming and subsequently extended the analysis to the Cabeza Prieta area in Arizona. Enhanced nighttime images, thermal-inertia images based on our new algorithm, and several profiles of various data across the basin are presented in our analysis and subsequently compared with other map data (geologic, magnetic field, known areas of oil, gas, and uranium occurrence, helium anomalies, and ground water). Of equal importance with the geologic interpretation has been progress in modeling. We provide several new algorithms: thermal-inertia mapping, estimation of regional meteorological information from the fundamental remote sensing data, registration of satellite day-night

images, elevation correction of thermal and thermal-inertia data, and determination of sensible-heat flux. The concluding section of this report addresses our image processing techniques together with a listing of the computer programs used.

2.1 GEOLOGIC SETTING

The study areas are the Powder River Basin and environs in eastern Wyoming-Montana and the adjacent Dakotas and the Cabeza Prieta Range in southwest Arizona. The Powder River Basin (lat. 42°-45° N., long. 103°-107° W.) has large potential for coal, oil and gas, and uranium, and accordingly is now the target of several major geologic, water-resource, and land-use mapping projects. Covering an area of about 250 x 400 km, it is a semi-arid region of rolling low hills typically with thin to moderate grass and sage cover. Tertiary rock units (Fort Union and Wasatch Formations) in the central area of the basin, where the energy resources are known to occur, are exposed on scales sufficient for satellite measurements. The lower part of the Fort Union is sandstone exposed in belts 4 to 10 km wide; the upper Fort Union part is siltstone with major coal beds exposed in belts 10 to 30 km wide; and the Wasatch is siltstone and claystone covering areas 30 to 60 km wide.

The Cabeza Prieta Range in Arizona (lat. 32°-33° N., long. 112°-115° W.) is a proposed Wilderness area, and the USGS has begun a program to define the geology and mineral-resource potential of this virtually unmapped area. The State geologic map shows the area to contain granite, schist, mafic volcanic rocks, and alluvium. It lies very near the major mineral district at Ajo, Ariz., and contains old prospect developments in hydrothermally altered

ground. Because the area has been withdrawn from public access since World War II, the geology and mineral potential are barely known and thus the area is considered relatively important for modern study.

2.2. APPROACH

Initial data interpretation was performed by visual pattern recognition of areas significantly different than their surroundings. Several 1:1,000,000-scale photographic enlargements were made of the NASA thermal and reflectance images to match them to many of the other existing data map products (geologic, geophysical, topographic, Landsat lineaments, and so on). Because of the X-Y distortion and the large magnification, this method was not entirely satisfactory for detailed study. We then generated film products from the computer-compatible tapes (CCT's) and used a zoom transferscope with X-Y stretch capability to register the projected images onto a stream-network map. In most local areas, this permitted plotting of features to within one to three pixels of their true ground position. Few of the interpretations based on the temperature boundaries or on other features are significantly affected by this degree of mislocation.

During this stage of the investigation, we also discovered that the NASA-supplied ΔT and thermal-inertia images contained artifacts, such as double drainage, indicating misregistration in parts of these images of several to many pixels. Consequently we developed a registration algorithm (Watson and others, 1981b) which registers data to within two pixels. Also as part of the investigation, we developed a new thermal-inertia algorithm (Watson, 1981a) which was employed during the remainder of our analysis. Correlation of these

registered image products with the other geologic-geophysical data was performed primarily by using optically enlarged projections of the data on digitally enlarged image product at a scale of approximately 1:200,000. This enabled us to examine subtle features at the pixel level and also to employ our full profiling and histogram capability at the full dynamic range and resolution of the digital image data. We have thus been able to quantify many of the scene differences which had been observed on various image products.

We also examined the use of color-coded images for enhancing subtleties in the scene contrast. Generally this provided a more obvious demonstration of differences but did not appear to add any new information. Toward the end of our study, however, a color-coded thermal-inertia image was produced which provided a new - if unexplained - perspective of the scene. A north-northeast-trending rectangular pattern of ground, surrounding the Black Hills and roughly corresponding with major changes in the drainages of the Yellowstone and Missouri Rivers was observed In retrospect, this feature can now also be seen on the black and white products. The color-coding of the image was also a very useful tool for quickly determining the numerical range of values. With an appropriate color-scale and using a high-powered magnification lens, it was possible to determine the thermal-inertia ranges of many geologic units quickly. In both these respects the color-coding can be regarded as a useful but not essential element in the analysis.

2.3 RESULTS

2.3.1 Thermal-inertia mapping for discrimination of geologic features

2.3.1.1 Delineation and subdivision of geologic units

Discrimination studies have been somewhat limited by the lack of sequential day-night image pairs free of major atmospheric/weather problems, but the 20 August 1978 set of day (AA0116-20010-1,2 and AA0116-20020-1,2) and night (AA0116-09040-3) scenes and our constructed temperature-difference (ΔT) and thermal-inertia images show several geologically significant features. Other good nighttime data from 30 July 1978 (AA0095-09170-3), 5 September 1978 (AA0132-09050-3), 27 September 1978 (AA0154-09190-3), and 10 June 1979 (AA0410-08450-3) passes have been used for delineation of several geologic boundaries, including some not within the area of, or not identified in, the 20 August 1978 data set.

A measure of discrimination capability, using optimal images and selection of geologic units which contrast well with their surroundings, is the clear delineation of the Mesaverde Formation. South of the Bighorn Mountains, in the vicinity of the towns of Midwest and Edgerton Wyo., the Mesaverde - a relatively massive sandstone - crops out between the Fox Hills Sandstone and the Cody Shale. On the night image (fig. 1) for 30 July 1978, all three units are relatively warm; however, the Mesaverde can be traced as a distinctly warmer unit ($1/4^{o}$-$1/2^{o}$ C), along at least 40 km of strike length in which a fold nose is clearly defined (fig. 2). The Mesaverde outcrop here is 1-2 km wide or 2-4 resolution elements (pixels).

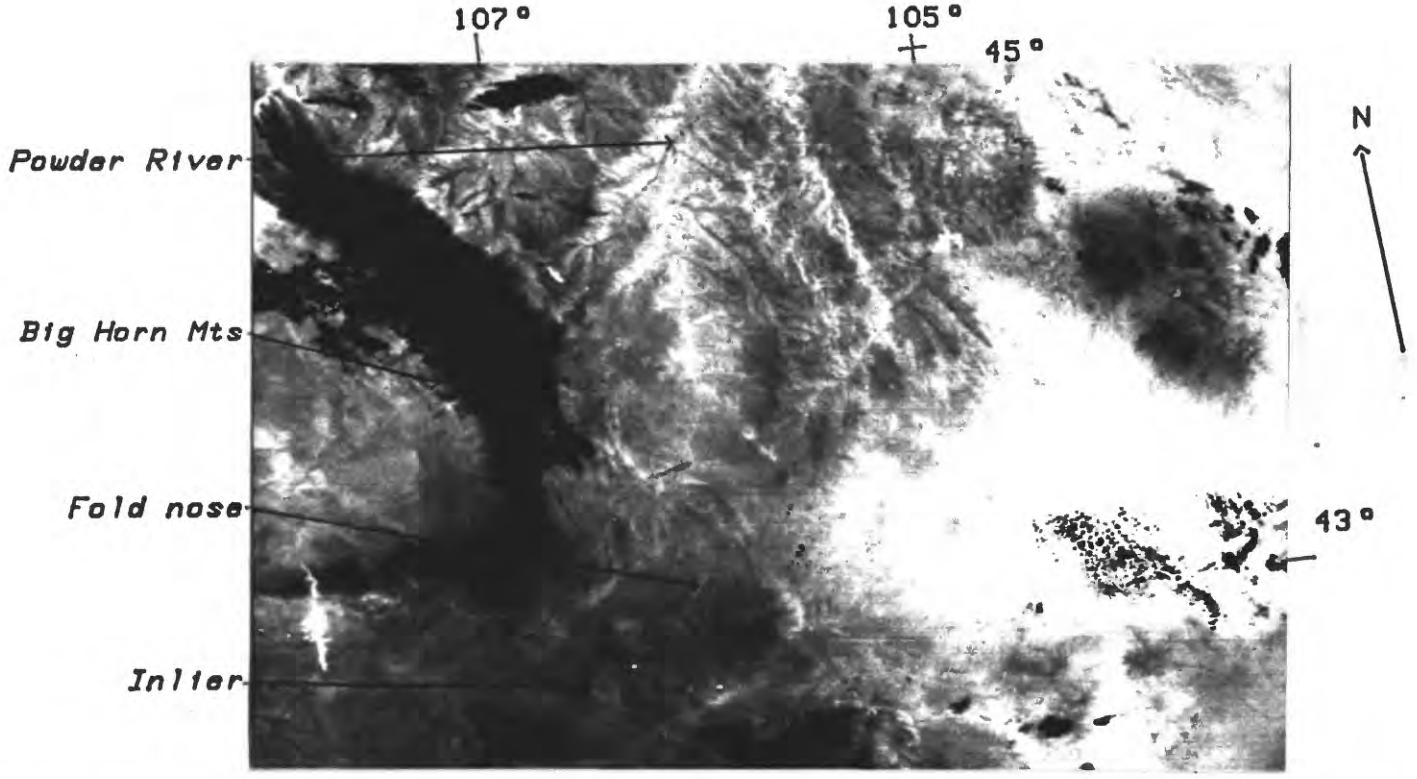

Figure 1.-- Night thermal image, July 30, 1978, of the Powder River Basin, Wyo., delineating the fold nose of the Mesaverde and the Frontier inlier. The standard convention of dark for low values and light for high values is employed on all images in this report.

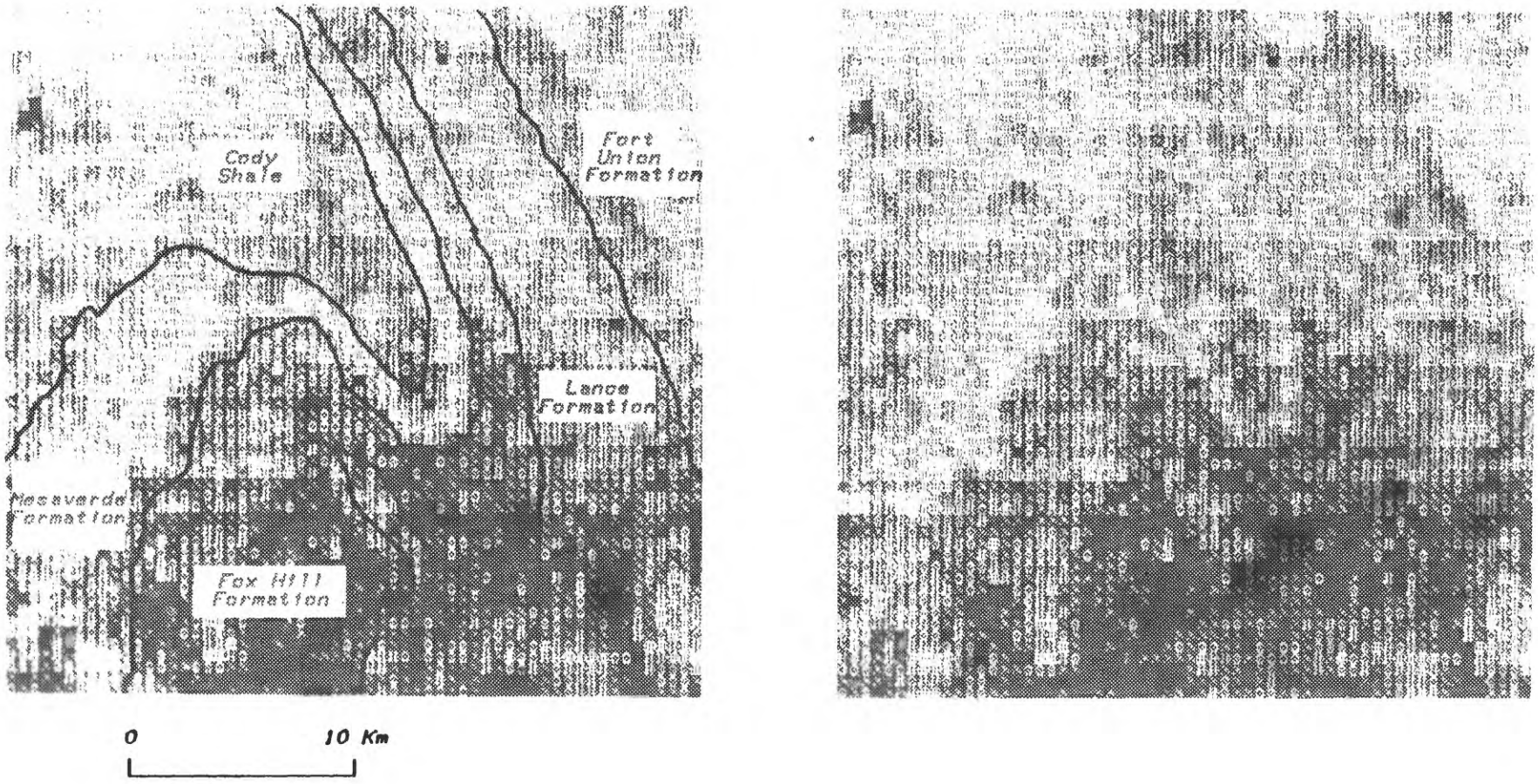

Figure 2.-- Fold nose of the Mesaverde Formation as expressed on the July 30, 1978, nighttime HCMM image. An unmarked image is provided for comparison.

Southwest of that area, south of the town of Powder River, within a large area of Cody Shale, is a sandstone inlier of Frontier Formation surrounding older shale and sandstone of the Cloverly and Morrison Formations. In the 30 July image, the Frontier is clearly a warm annulus around a cool center of the other units (fig. 1 and 3). The units in the cool central area are about 5 km wide and the warm Frontier annulus is 3.5 km wide. What is additionally interesting in this area is the apparently clear definition of a similar but smaller such feature to the northwest which does not match the shape of the contacts on the most recent geologic map (Love and others, compilers, 1955). This feature has not been field checked.

Another measure of discrimination is found in the area of the Pumpkin Buttes. These are very sharply defined in the 5 September 1978 night image (fig. 4). North Butte is about 3 km wide, and the combined topographic/geologic prominence of Middle and South Buttes measures about 4 by 8 km. These are warmer than their surroundings, as is expected of tuffaceous sandstones of the White River Formation, dense and resistant enough to form buttes where erosional remnants lie upon the softer sandstones and mudstones of the Wasatch Formation. Once again, when the geologic map was projected onto this HCMM scene, differences were observed. Unfortunately, on our only thermal-inertia image, clouds were present over the Buttes preventing the observation of the expected thermal-inertia contrast.

Definition of geologic features is highly variable from pass to pass and within single passes. The 30 July image (fig. 1) is excellent for the north half of the Powder River Basin and the areas west and southwest of the Basin. The image appears virtually washed out in the south half of the Basin,

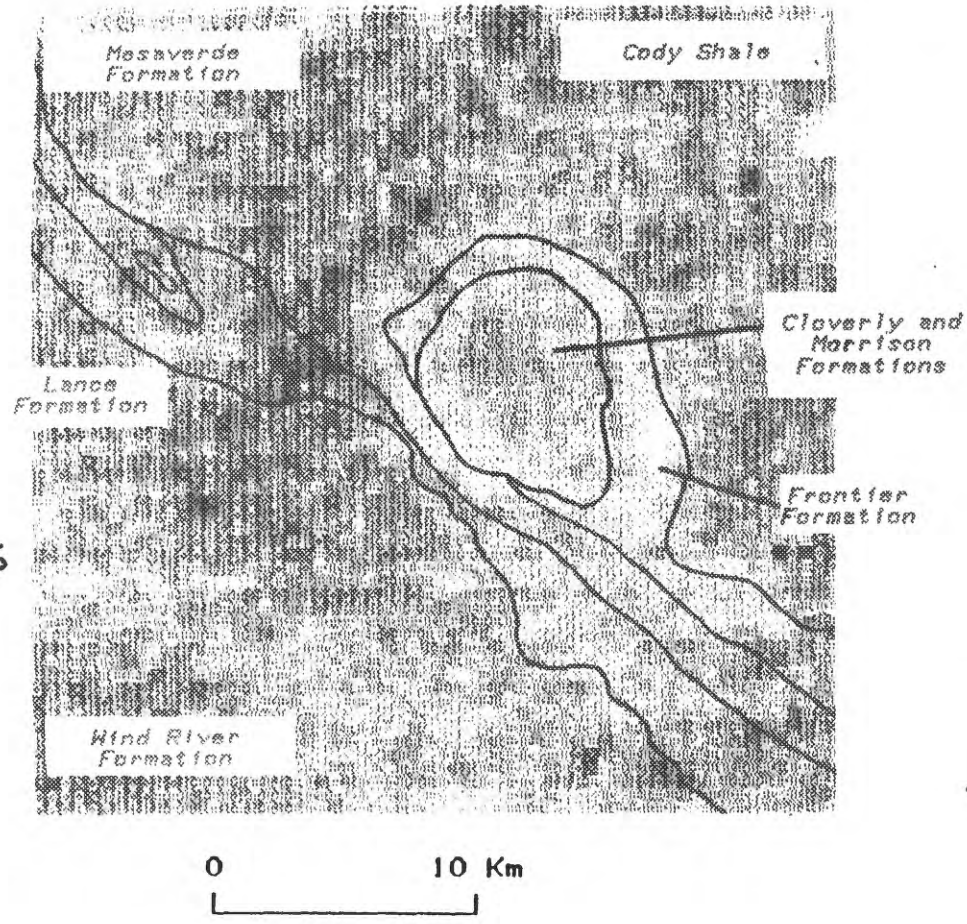

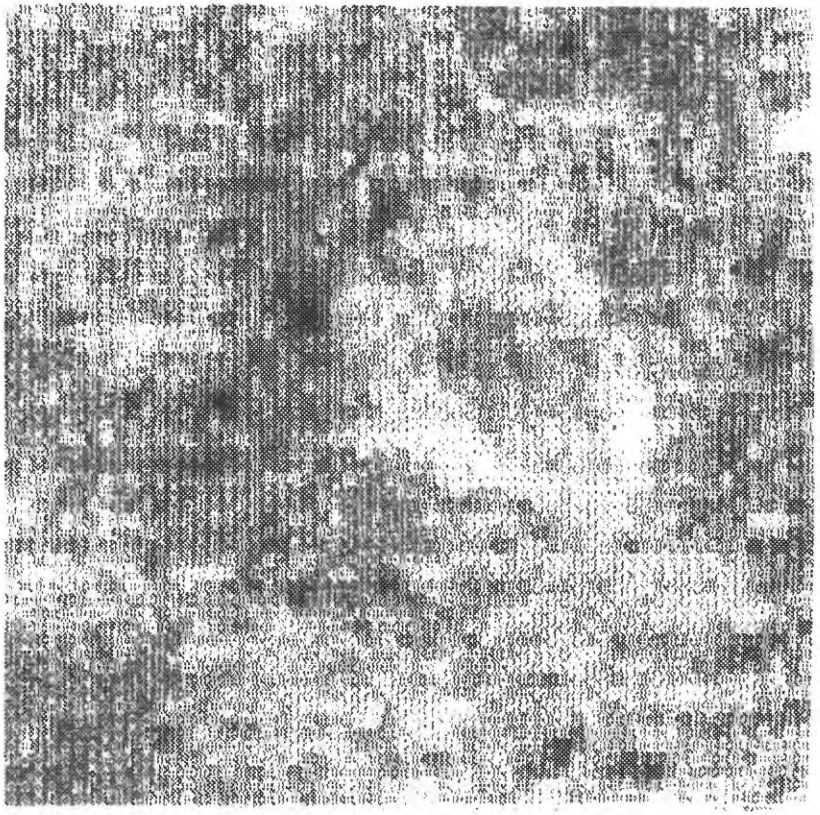

Figure 3.-- Inlier of the Frontier Formation as expressed on the July 30, 1978, nighttime HCMM image. An unmarked image is provided for comparison.

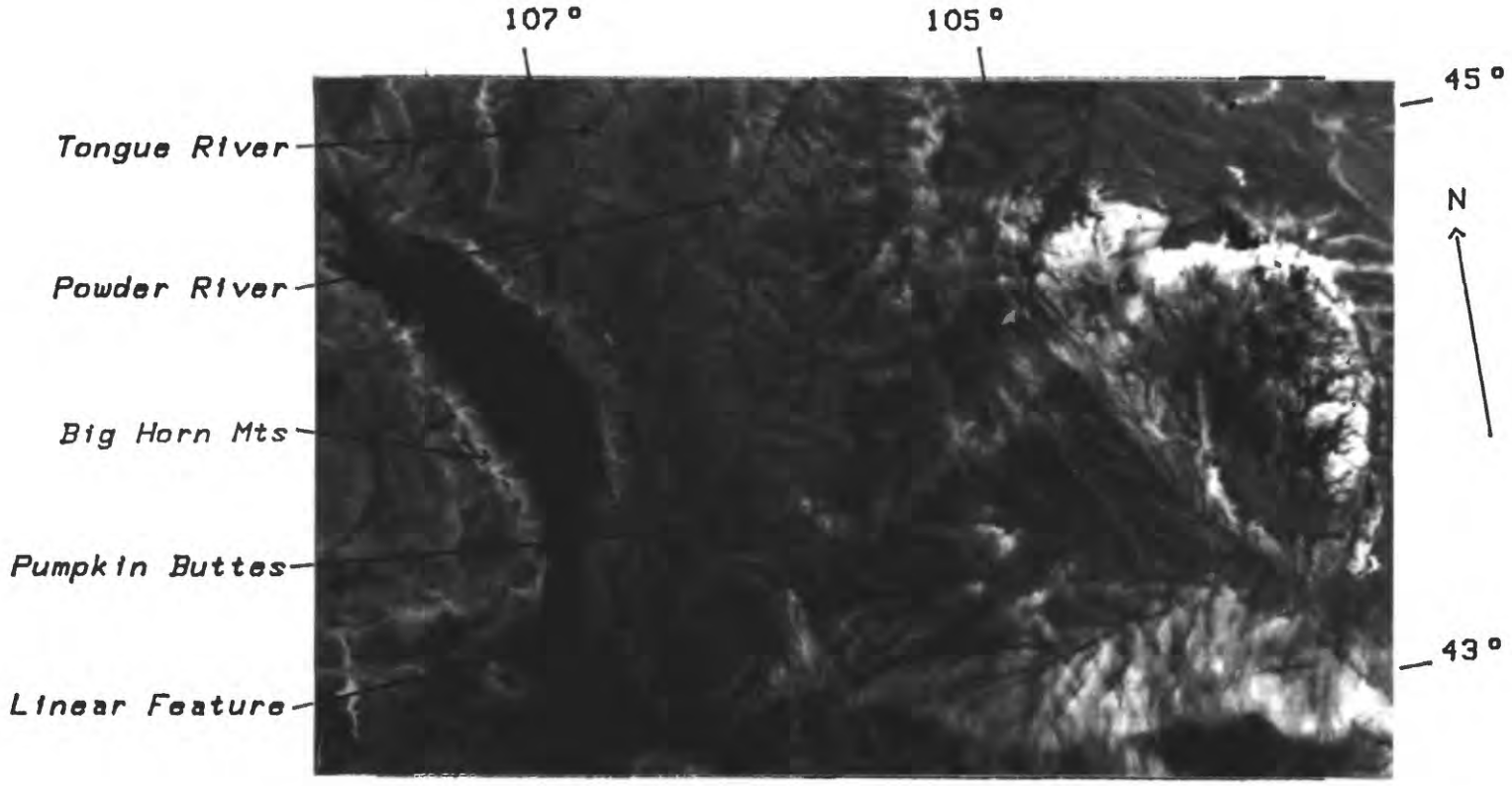

Figure 4.-- Night thermal image, September 5, 1978, of the Powder River Basin, Wyo., showing the descrimination of the Pumpkin Buttes.

showing high temperatures in an area conspicuously cool in all the other images. Because the image was examined long after it was acquired, it was not possible to obtain detailed field meteorological data. This is a generic problem in dealing with transient and local phenomena that commonly affect thermal surveys. Air temperature and precipitation data show fairly similar conditions at the 28 weather stations throughout the scene. From these data, the intrascene variations cannot readily be ascribed to local weather/moisture changes; however, the NOAA and DMSP (Defense Meteorological Satellite Program) Satellite data show that a major weather front had recently passed through the basin. Such intrascene differences are less pronounced or even absent in other passes, but none of the others expresses quite the same degree of geologic feature definition as the good portions of the 30 July image.

The multiple data sets of 20 August contain considerable geologic information, especially in comparing patterns seen variously in the day thermal, night thermal, ΔT, and thermal-inertia images. The day thermal image (fig. 5) shows large areas of warm ground north and east of the Black Hills. These do not correspond to lithologic subdivisions on any available geologic maps, nor to any patterns of weather across the scene during the previous few days. Small individual features of interest in the image are cool areas around the Tongue River and in a belt of small patches trending north-south up the center of the southern part of the basin. The very warm drainage area west of the Black Hills and the warm area south of the Black Hills are also noteworthy. The night image (fig. 6) offers busier patterns of finer scale definition, dominantly related to the topographic character of local areas. Much, but not all of the high ground between streams, is conspicuously warm. The long,

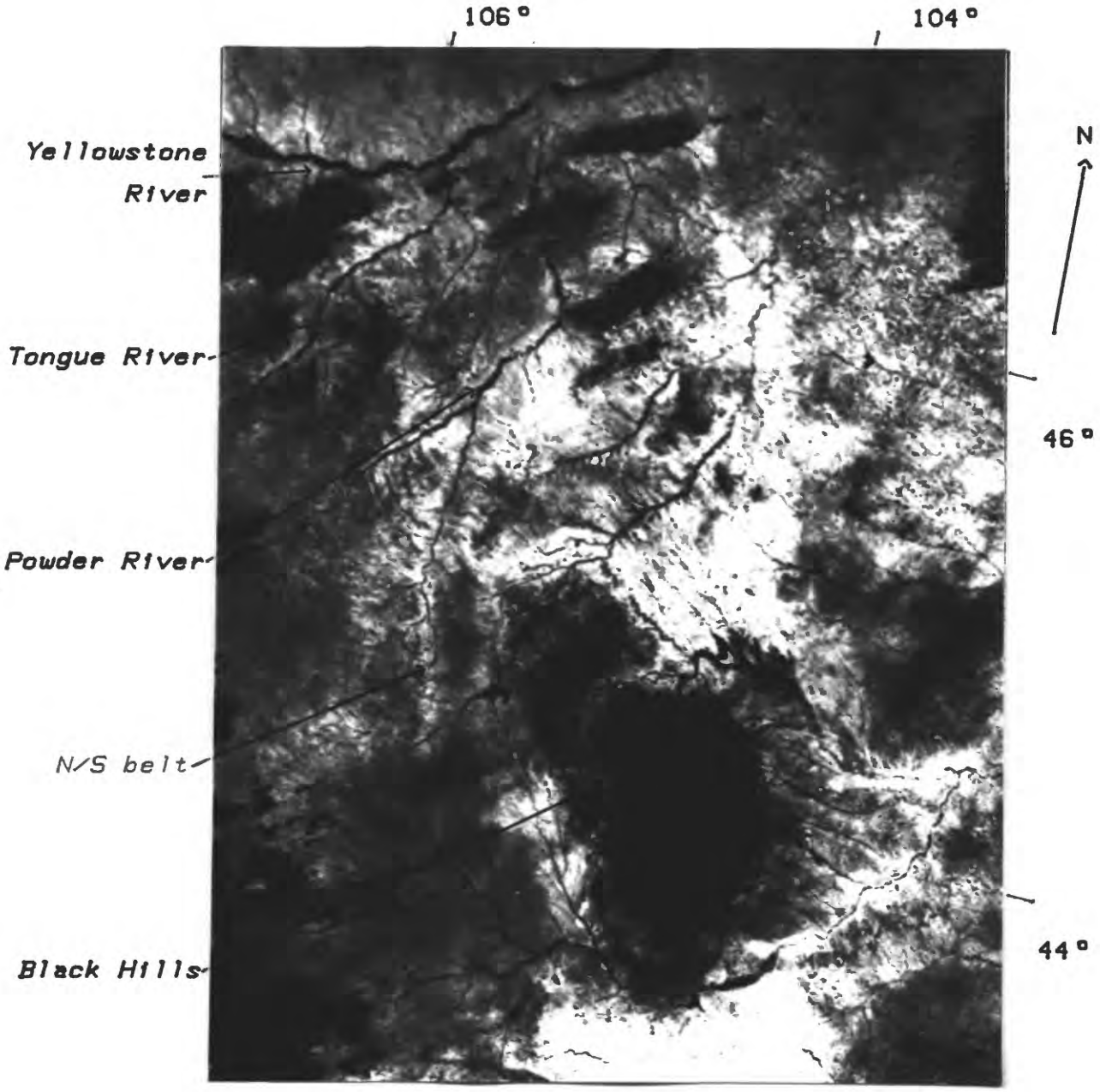

Figure 5.-- Day thermal image, August 20, 1978, of the Powder River Basin, Wyo., showing thermal boundaries.

0 100 Km

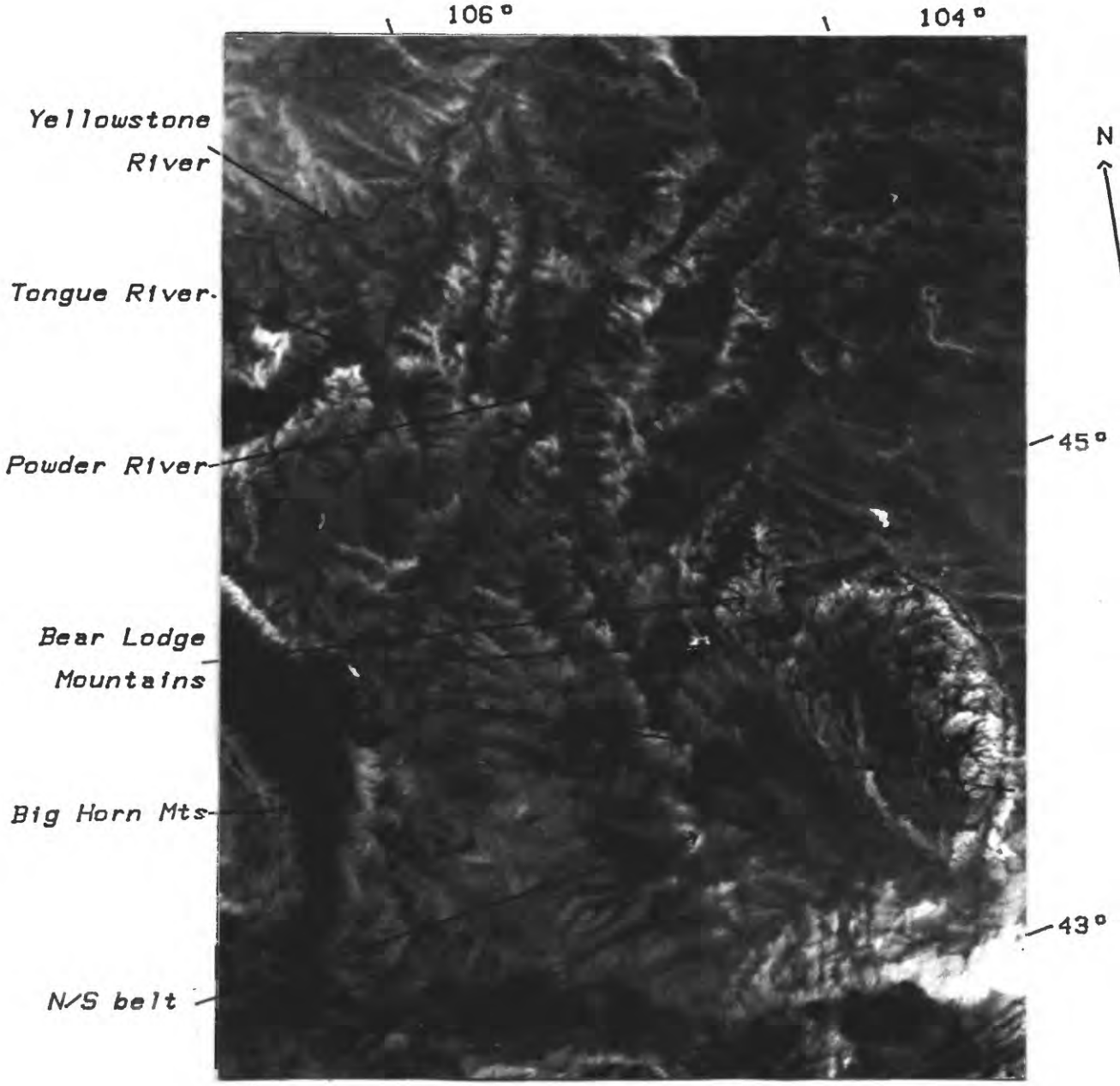

Figure 6.-- Night thermal image, August 20, 1978, of the Powder River Basin, Wyo., showing the conspicuously warm areas. The unlabeled lines are profiles A-A′ (north line) and B-B′ (south line).

0 100 Km

straight Powder River separates warm ground on its east flank from cooler ground on its west flank. This is not just an effect of east- vs. west-facing slopes, because most other stream areas do not show the same effect. The north-south belt in the southern part of the Basin shows as very warm patches of ground. Very warm areas ring the east flank of the Black Hills and occur just to the north throughout the Bear Lodge Mountains, but these do not correspond to the mapped geology. Other contrast stretches were tried including color slicing but the correlations of temperature areas with geology did not improve. What does appear to be true, however, is that within the Powder River Basin, conspicuously warm areas are much more abundant in the north half. For the most part, this is a result of greater dissection of the terrain and more exposure of bedrock, as compared with few outcrops and abundant windblown sand veneer in the south half.

Analysis of the thermal-inertia images, derived from our registration and modeling algorithms, showed that the Tongue River areas of cold ground in daytime are, in fact, areas of high thermal inertia (2000 Thermal inertia units (TIU); 1 TIU = 1 W $sec^{1/2}$ m^{-2}). These areas (fig. 7) correspond quite well to areas mapped by Raines (Raines and others, 1978), using computer enhancements of Landsat images. They were mapped as the coarsest, sandiest lithofacies unit in the basin, which are relatively indurated and resistant and should crop out best and, depending on moisture conditions, should have the highest thermal inertia of the subunits in the Wasatch and Fort Union Formations. Other such correlations exist for several areas of this facies southeastward toward the Black Hills. Areas of the Wasatch and Fort Union, sampled from various parts of the Basin and which appear to be representative

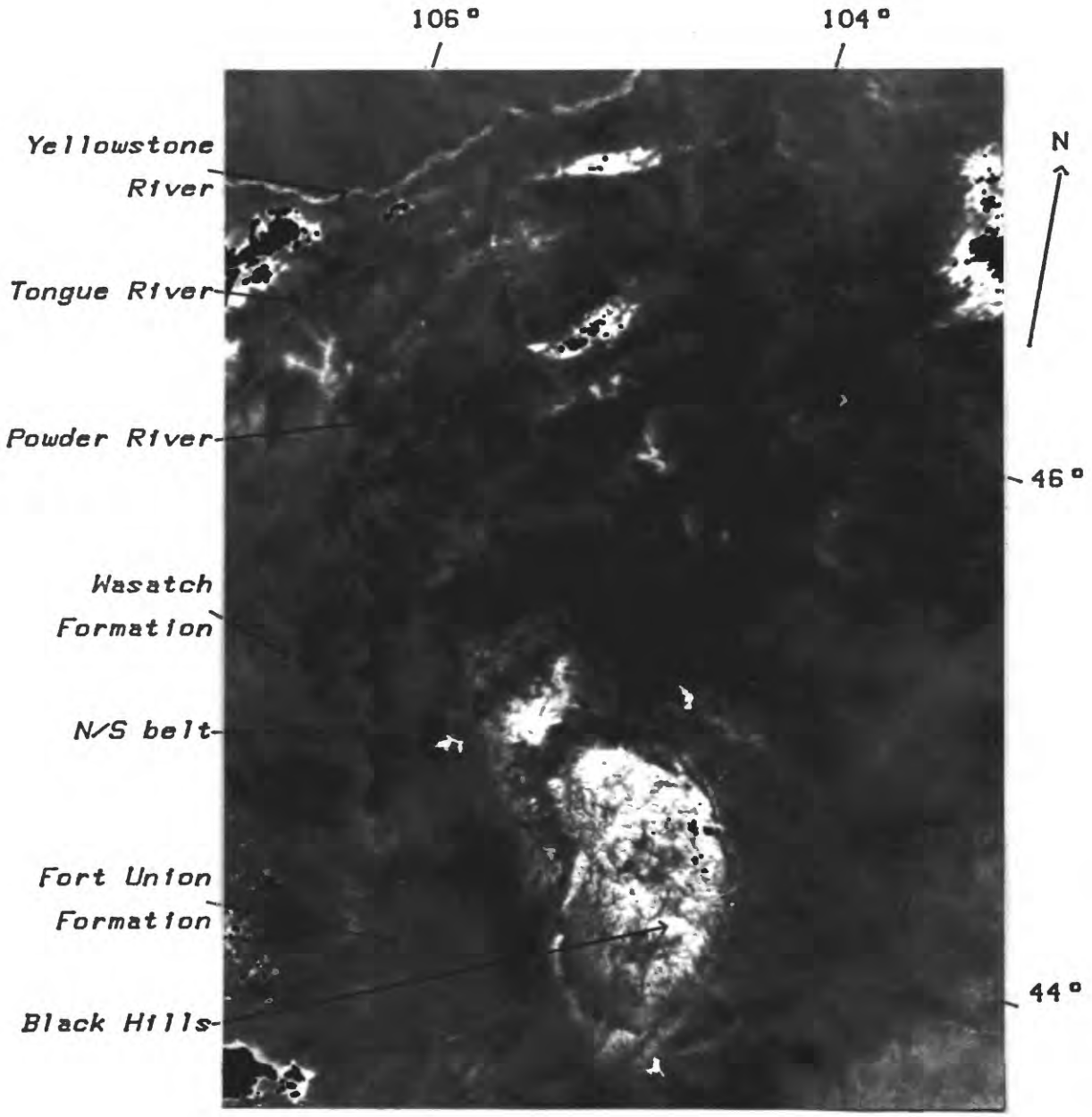

Figure 7.-- Thermal-inertia image, August 20, 1978, of the Powder River Basin, Wyo.

of larger surrounding areas have thermal-inertias of 1525 TIU and 1450 TIU, respectively. However, the thermal-inertia of these two units varies considerably throughout the basin and in some cases values for these two units are statistically inseparable. A possible explanation is that these units generally form low or flat topography where windblown sand obscures the underlying geology in extremely irregular (and unmapped) patterns. Another reason is that these units retain moisture differently and longer than sandier facies, and thus may have great irregularities in both thermal-inertia values and wind cooling patterns. If they are slightly wet, and not cooled by surface winds, their thermal inertia will be higher.

The north-south belt of high thermal inertia (fig. 7) was initially thought to correspond to burned ground over ancient natural coal fires. The night thermal image (fig. 4) was carefully registered to a base map and a composite map was made showing the areas of clinkers (as determined from a color ratio composite Landsat image) and the warm areas on the HCMM image (fig. 8a). We then examined the thermal-inertia image and determined that the clinker areas in fact have an intermediate thermal inertia (1300 TIU) and the N-S belt of warm ground in the night image just east of the clinker hills has a higher thermal inertia (1500 TIU). This north-south belt has been mapped in detail and the surface geology provides no clue as to why these areas have high thermal inertia. This does not conform with conditions produced where windblown sand accumulates in the lee of topographic highs. It is suspected that the highly fractured clinker hills are readily drained of their near-surface moisture and this ground water tends to pond just eastward in the direction of normal drainage, causing an increase in thermal inertia. This

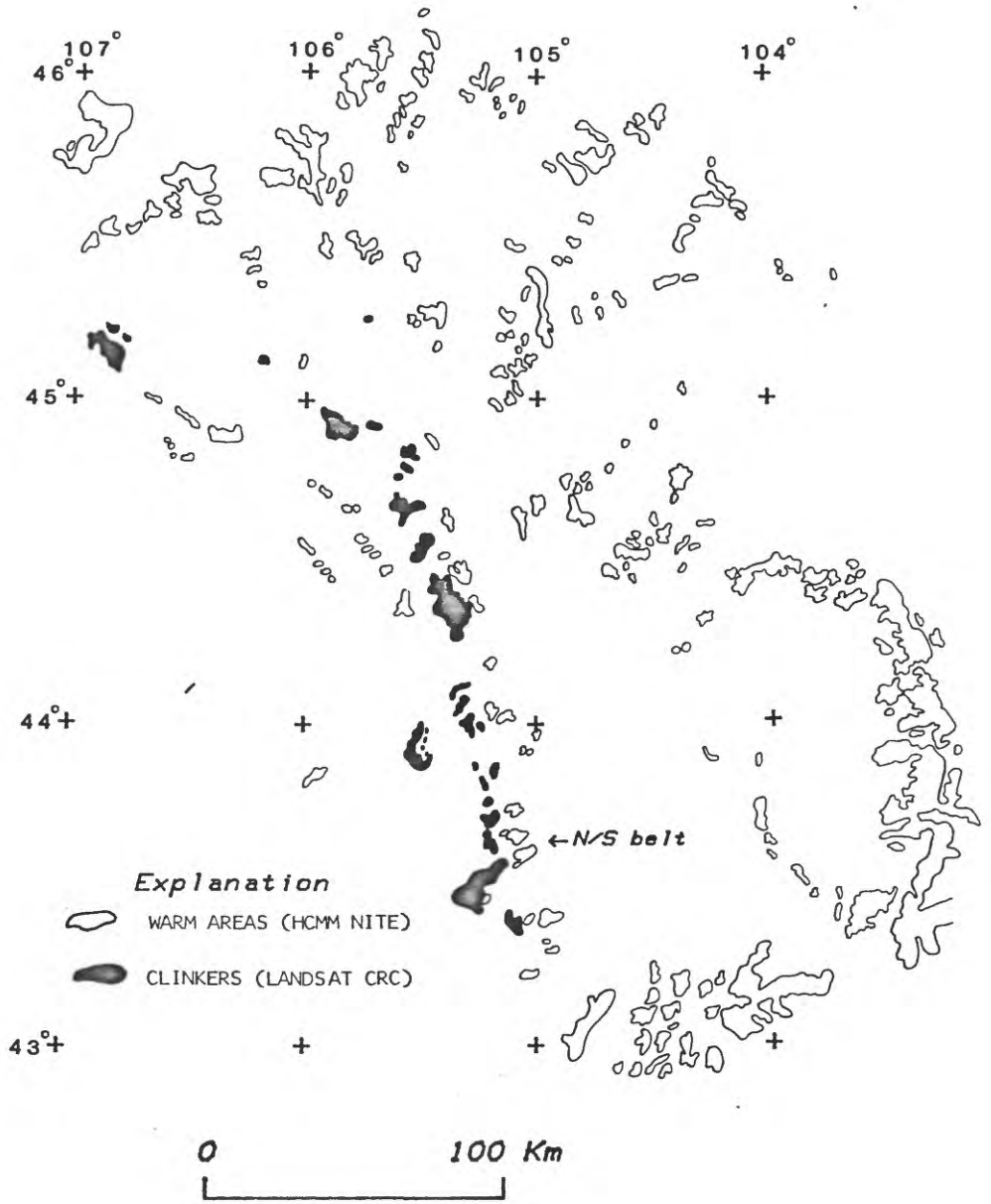

Figure 8a.-- Base map of the Powder River Basin, Wyo., showing the location of the clinkers with respect to the warm areas which have high thermal inertias.

hypothesis is given credence by an examination of the NURE gamma-ray profiles in this area. These areas coincide with lows in the total gamma-ray measurements (fig. 8b) as would be expected for areas of higher moisture content.

A rough order of magnitude estimate from these data is that the anomalous areas are associated with a 20 percent increase in thermal inertia and a 5 to 10 percent decrease in the total count values. The thermal inertia of soils increases rapidly with increasing soil moisture content and the effect can be estimated for low moisture contents by considering only that increase due to density and specific heat capacity. The ratio of the fractional change in thermal inertia to density is just one half the ratio of the specific heat capacity of water to soil or approximately 2.5. Thus a 20 percent increase in thermal inertia could be produced by a soil moisture change which increases the density by 8 percent (and decreases the total count by an equivalent percent).

To examine the basin further, two northwest-southeast profiles across the 20 August image (fig. 6, profiles A-A', B-B') were constructed. These profiles enabled us to look in detail (pixel level) at variations in thermal-inertia values and to examine relationships between temperature or thermal-inertia patterns and topography. Topographic data were taken from 1:250,000 USGS base maps with a contour interval of 200 feet. Figures 9 through 14 show profiles of thermal-inertia, elevation, and topographic gradient along lines A-A' and B-B'.

The profiles on A-A' have several interesting features. The line begins in the Wasatch Formation at the northwest end, and thermal-inertia values (fig. 9) decline into a broad low, about coincident with the Powder River

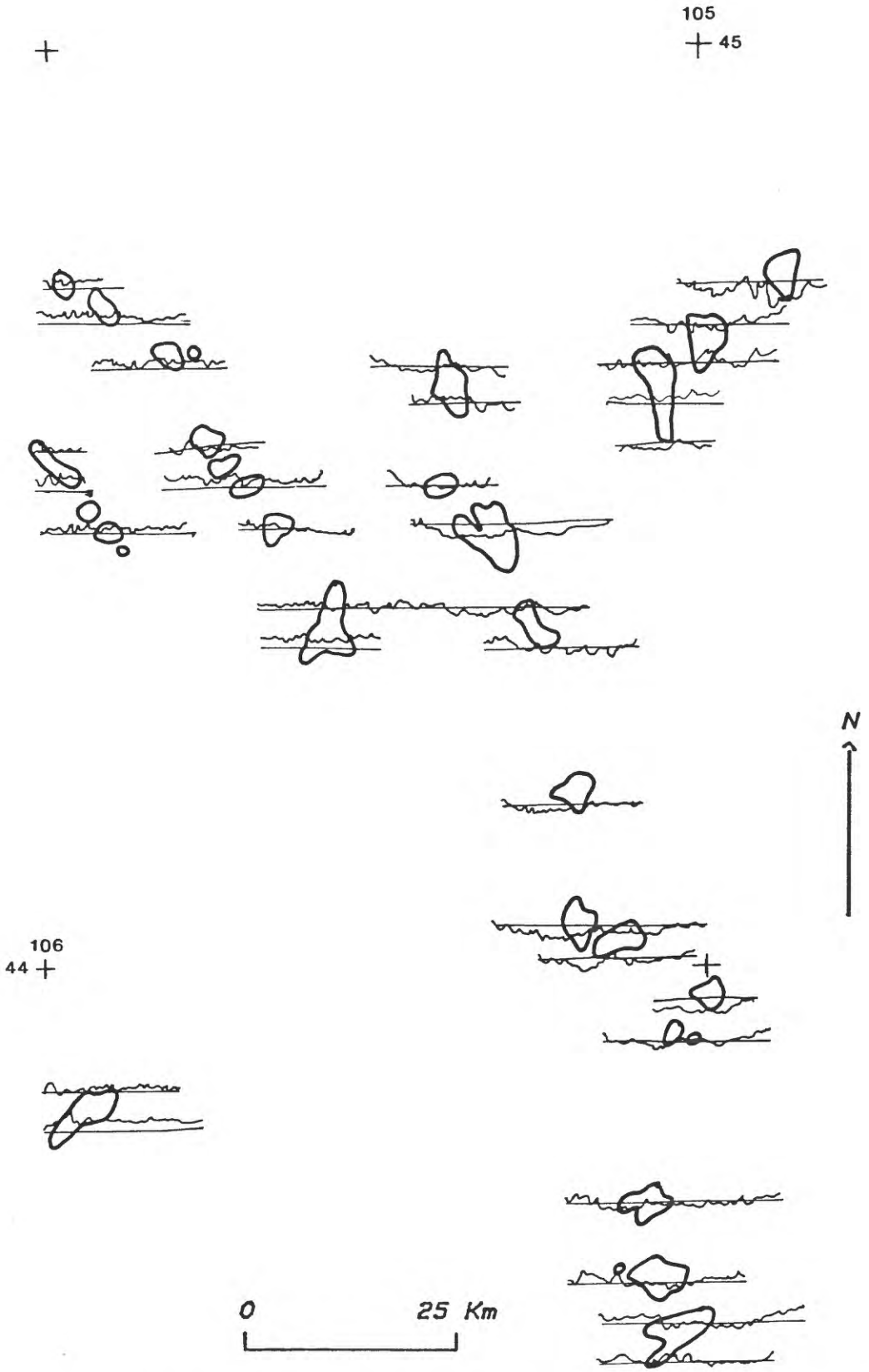

Figure 8b.-- Comparison between profiles of total count gamma ray and the anomalously warm areas. The straight lines indicate the geographic position of the profiles.

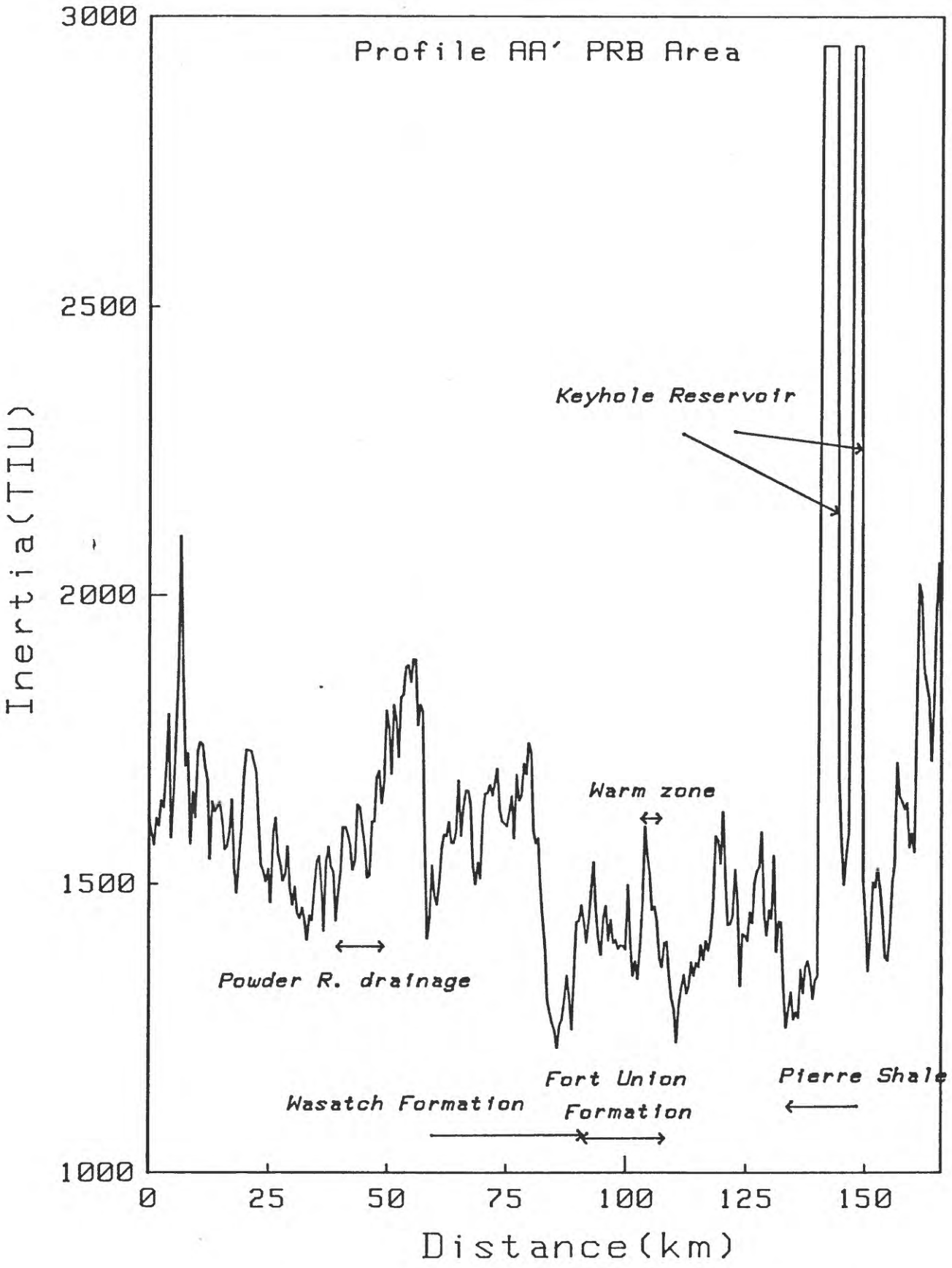

Figure 9.-- Thermal-inertia profile for line A-A'.

drainage seen so clearly in the topographic profile (fig. 10, 11), and then rise. This low approximately marks the basin axis, and the adjacent slopes of the thermal-inertia profile show the character of the upper part of the Wasatch on either side of that axis. The topography itself is somewhat different on opposite flanks of the Powder River drainage, and this probably explains the previous observation that the night-temperature image showed the two flanks differently, even though the thermal-inertia image indicated the two flanks to be underlain by similar material. The flanks have different slopes and bed dips, and the western flank generally is dissected more sharply and deeply than the eastern flank. At the next large drainage east of the Powder River, the thermal-inertia profile breaks sharply, suggesting either a previously unmapped lower unit of the Wasatch or a sharp change to the somewhat finer grained facies which has been noted in the lower part of the formation. Along this profile the Fort Union Formation has a roughly estimated average value of 1425 TIU, as compared with an equally rough, general average of the Wasatch of 1625 TIU. This difference is about what would be expected from the compositions of the two formations, although they are rather nonuniform on the scale of the whole basin. The "typical" areas of Fort Union and Wasatch that were sampled gave values of 1450 TIU and 1525 TIU, respectively. A sharp break in the thermal-inertia profile occurs between the two formations, but it falls 4 to 5 km west of the contact as shown on the geologic map. A break or dip also occurs in the profile at the contact of the upper (Lebo Shale) and lower (Tullock) members of the Fort Union, but overall the members have about the same thermal inertia. The elevation profile shows a marked change in character of topography from Wasatch to Fort Union, as does

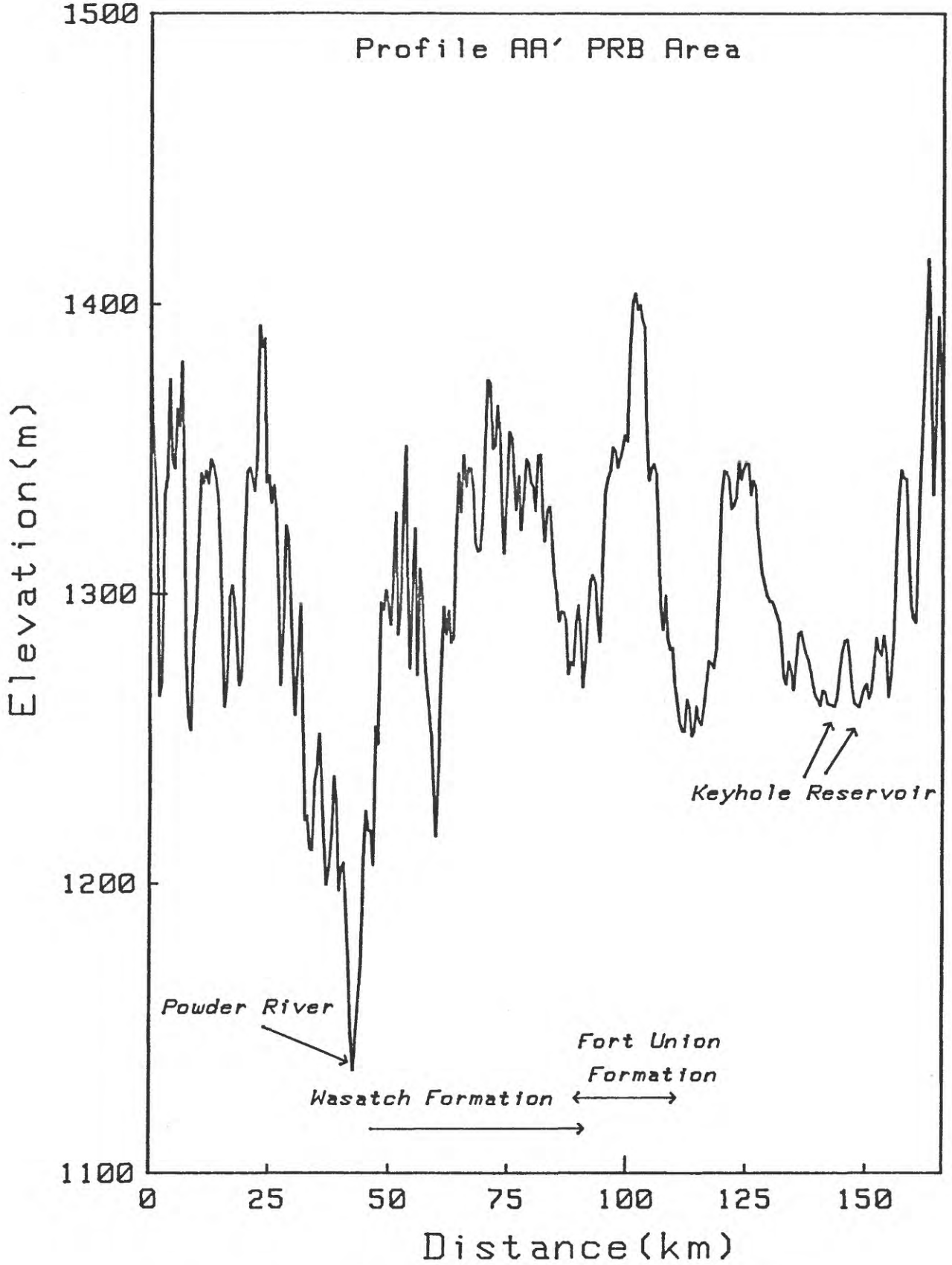

Figure 10.-- Elevation profile for line A-A'.

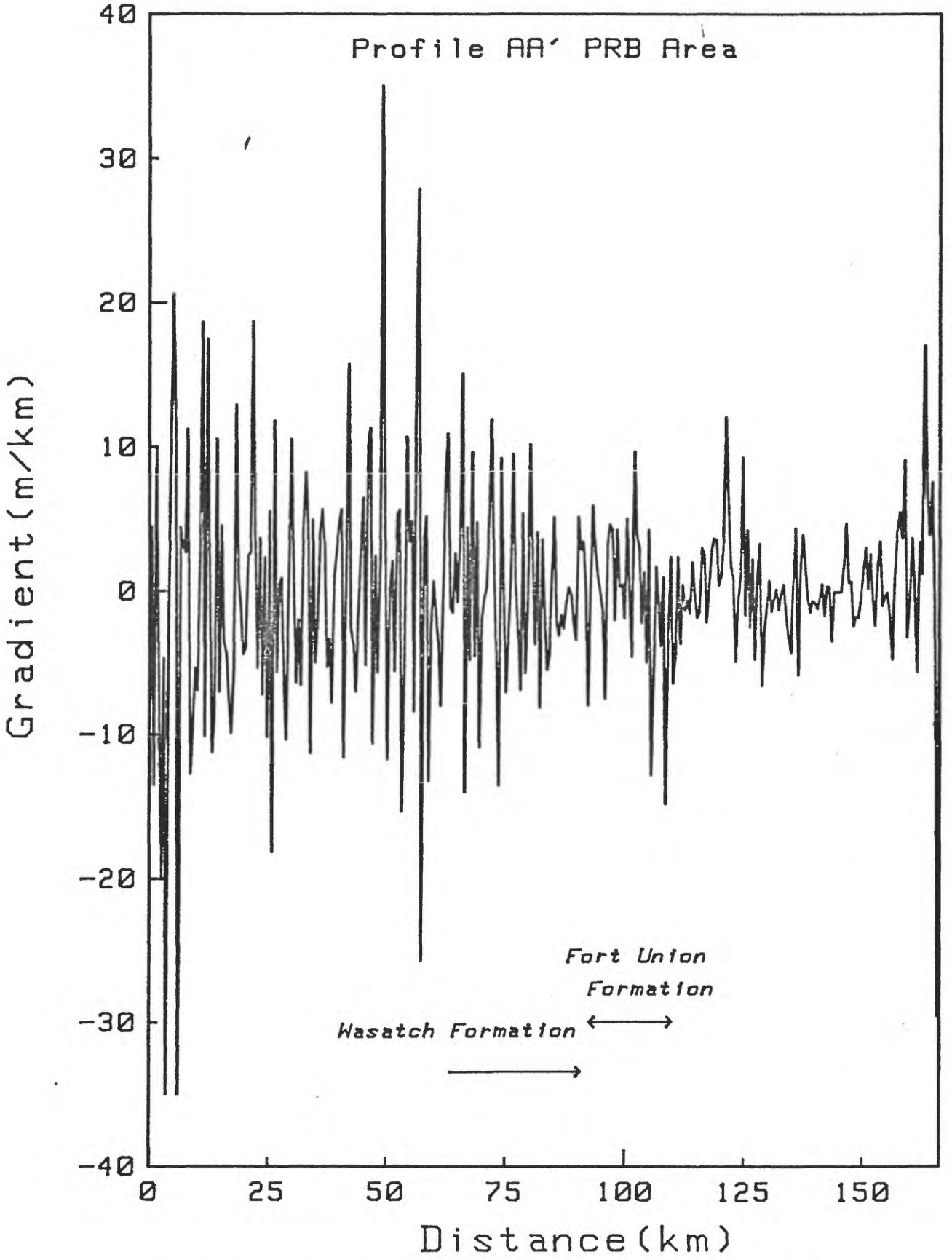

Figure 11.-- Topographic-gradient profile for line A-A'.

the topographic-gradient profile. The warm north-south zone is a narrow but prominent thermal-inertia spike in the lower part of the Lebo Shale Member of the Fort Union. The Pierre Shale has the lowest thermal-inertia of any units along the profile (about 1330 TIU), in huge contrast with the adjacent spikes which mark Keyhole Reservoir.

Line B-B' presents a rather different character in the profiles. The Wasatch thermal inertia (fig. 12) is not at all like that on line A-A'; most of its width on line B-B' is an area of unexplainedly low values which mark a very distinctive and nonrepresentative area within the widespread formation. Wasatch with relatively normal-appearing thermal-inertia image character appears next to the cloud area at the northwest end of the line; there its estimated average thermal inertia is 1550 TIU, only 5 percent different from that seen on line A-A'. The area of low values does not appear to be related to microclimatic factors, nor to any geologic feature of which we are aware. For example, neither here nor elsewhere in the image area do thermal-inertia values closely and consistently correspond with the inferred lithofacies areas delineated in Landsat images. On this line, the Lebo Shale Member of the Fort Union has a roughly estimated thermal inertia of 1750 TIU, higher than the representative Wasatch values. Most of this is in the broadest part of the north-south warm zone, however, so the values almost certainly do not represent normal character. The Tullock Member of the Fort Union is estimated at 1300 TIU, almost 10 percent lower than the Fort Union of line A-A'. Such a change is believed to be both real and significant in terms of the geology, but no data are available as to possible lithologic changes of the unit between the two profile areas. The Pierre Shale has a thermal inertia of 1260

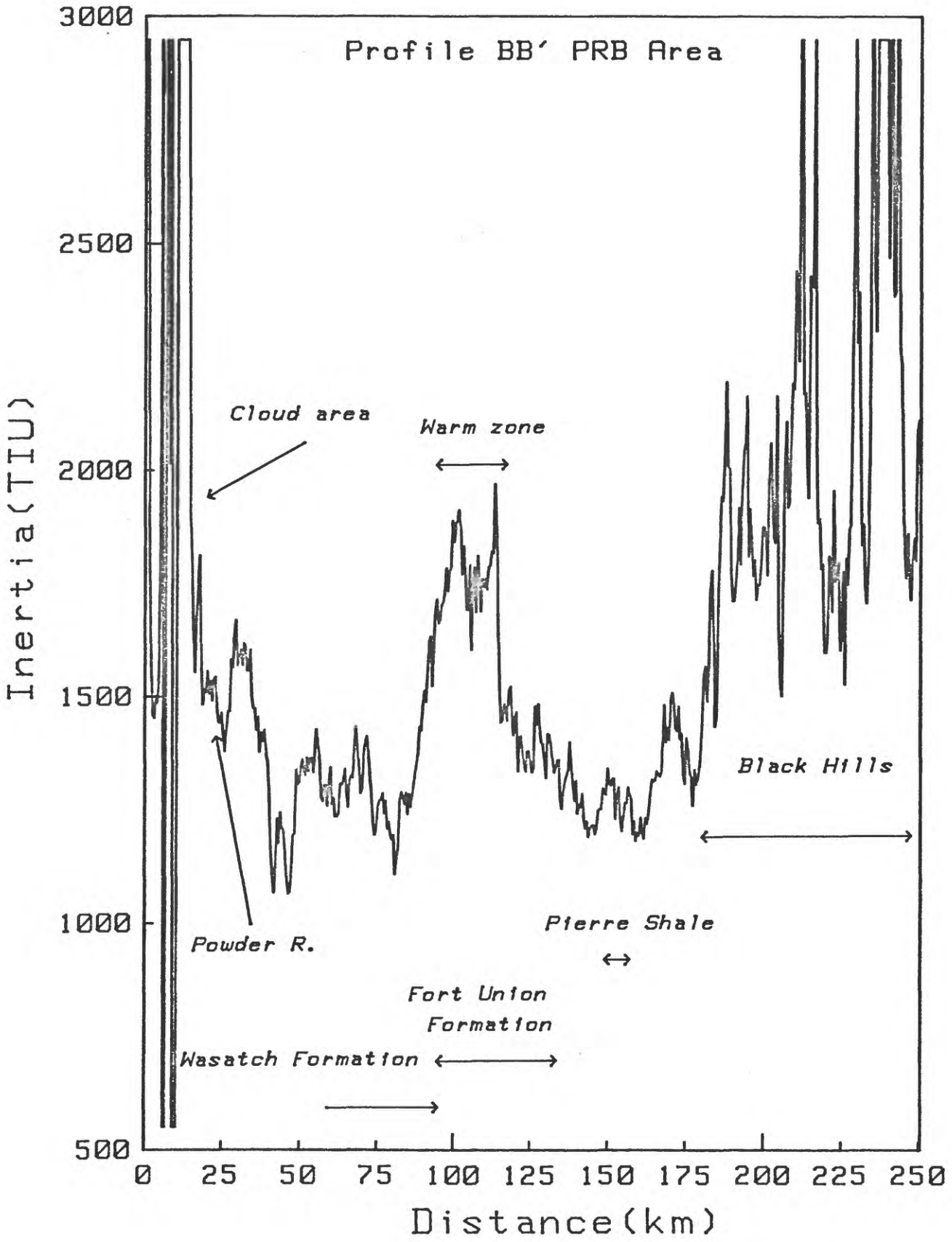

Figure 12.-- Thermal_inertia profile for line B-B′.

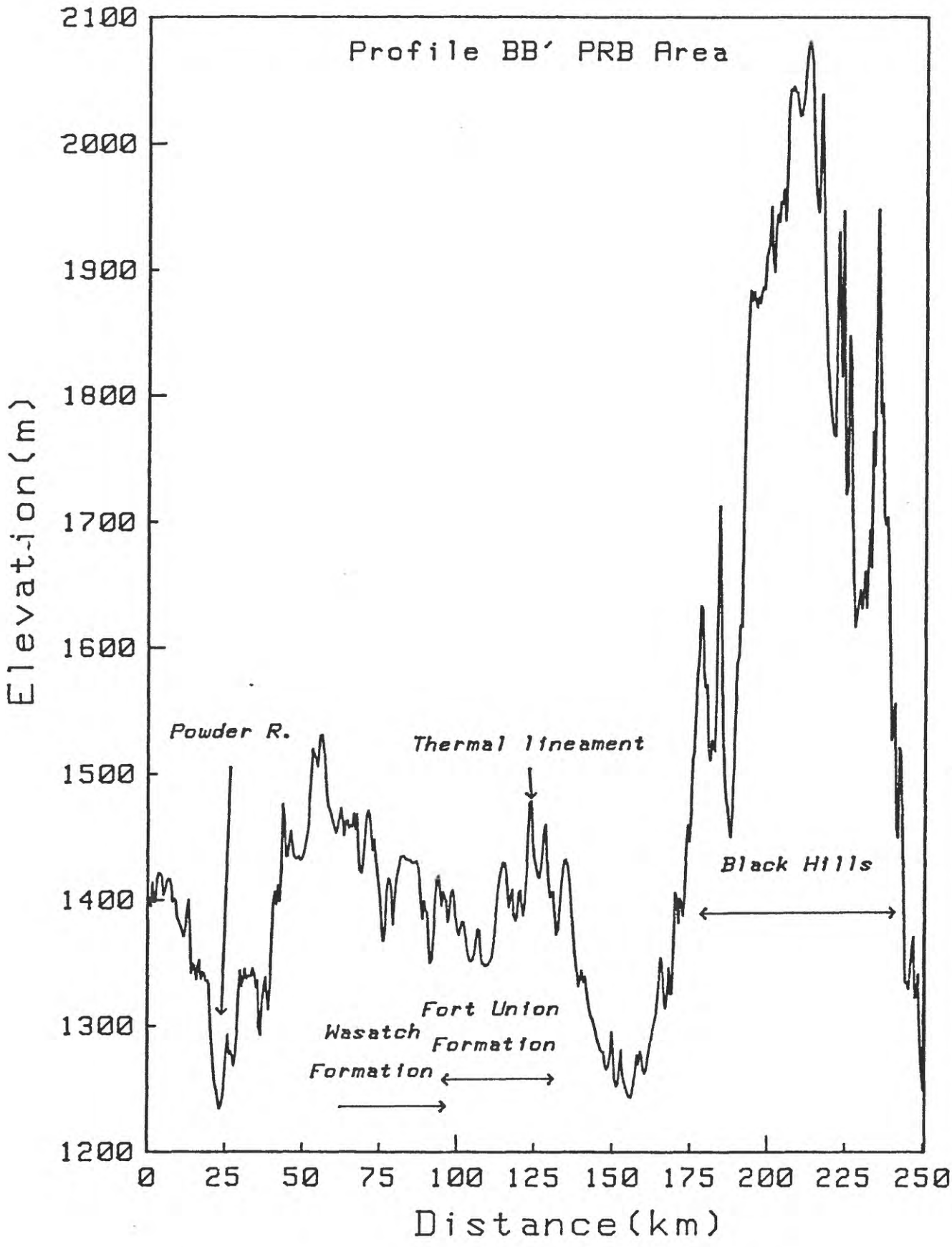

Figure 13.-- Elevation profile for line B-B'.

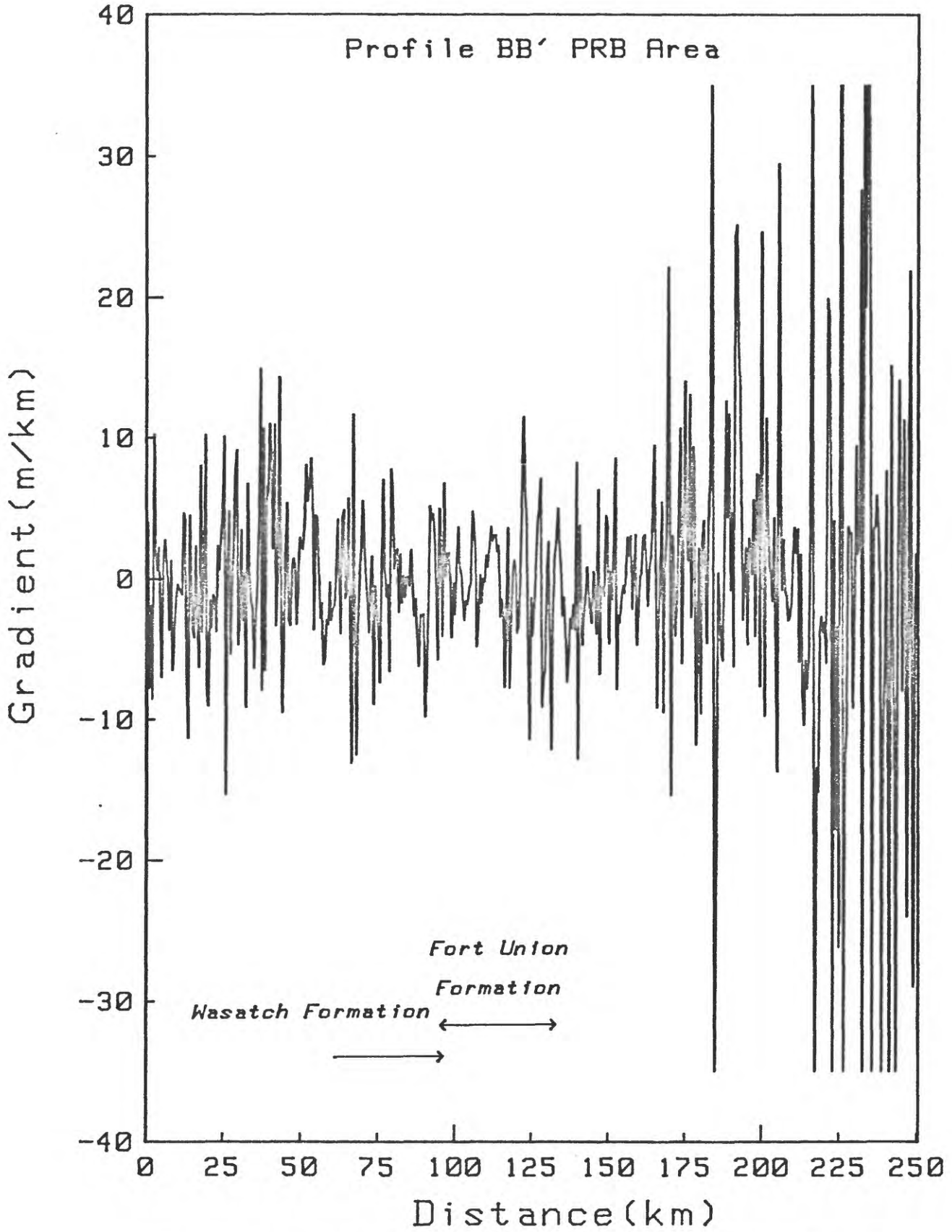

Figure 14.-- Topographic-gradient profile for line B-B′.

TIU, about 5 percent less than observed on line A-A', and again the lowest values of any geologic units on the profile. High and highly variable thermal inertia is seen in the Black Hills portion of the profile as expected in an area of alternating high vegetation density and bare rock exposures.

From this analysis, it appears that thermal data, especially when coupled with topographic information, can aid materially in discriminating geologic formation and member differences, even (as in the Powder River Basin) where units are so variable and exposures so poor that geologists have had real problems or have been unsuccessful in such efforts. It appears that thermal-inertia differences of perhaps as little as 5 percent, and certainly 10-15 percent, can be delineated and used in mapping, probably in terms of both rock units and generalized soils characteristics. So far, patterns seen in thermal-inertia images do not match with vegetation patterns seen in Landsat images and believed to correspond to subtle facies differences. This problem needs further investigation; it may relate to difference in resolution of the two satellites and to differences in depths "seen" by thermal-inertia measurements and vegetation root systems.

2.3.1.2 Geomorphic domains and linear features

An interesting and important aspect of using thermal-inertia images is that erroneous impressions gained from temperature patterns are corrected and a truer picture of surface properties obtained. This is particularly true of night thermal data. For example, the very warm zone around the Black Hills in the night image (fig. 6) disappears in the thermal-inertia image (fig. 7), and a whole new pattern emerges. The contrast of opposite flanks of the Powder

River also disappears, indicating no basic difference in geologic materials across the river. Thus we can use thermal, albedo, and thermal-inertia data in concert to separate physical properties differences (integrated over the top decimeter of the soil or rock profile) from those effects due to such parameters as slope, altitude, and surface reflectance.

For the units underlying most of the Powder River Basin, presently available thermal data and derived products show many unexplained patterns, some of which probably were due to transient (and now untrackable) atmospheric events. Others, however, are believed to reveal real differences in the geologic materials, but current maps in general do not offer a sufficiently detailed base for correlation. Certainly some correlations are found with Landsat-mapped lithofacies, but more day-night pairs covering varying moisture cycles would have been necessary to see through such "noise" as windblown sand, surface-wind cooling patterns, and local moisture variations.

Linear features, often long reaches of streams that appear straight at HCMM resolution, are readily defined in the night images. Many of these coincide with breaks or trends in contoured aeromagnetic data, suggesting that basement tectonic elements have printed through the thick sedimentary sequence to control stream courses. This implies that during sedimentation at earlier times, such features effected some control of sedimentary depositional patterns a conclusion recently elaborated for the Powder River Basin (Slack, 1981).

The most remarkable, previously unrecognized, linear feature appears prominently on the night image of 5 and 27 September (figs. 4 and 15) and also 20 August (fig. 6). Although it is not recognizable as a discrete linear

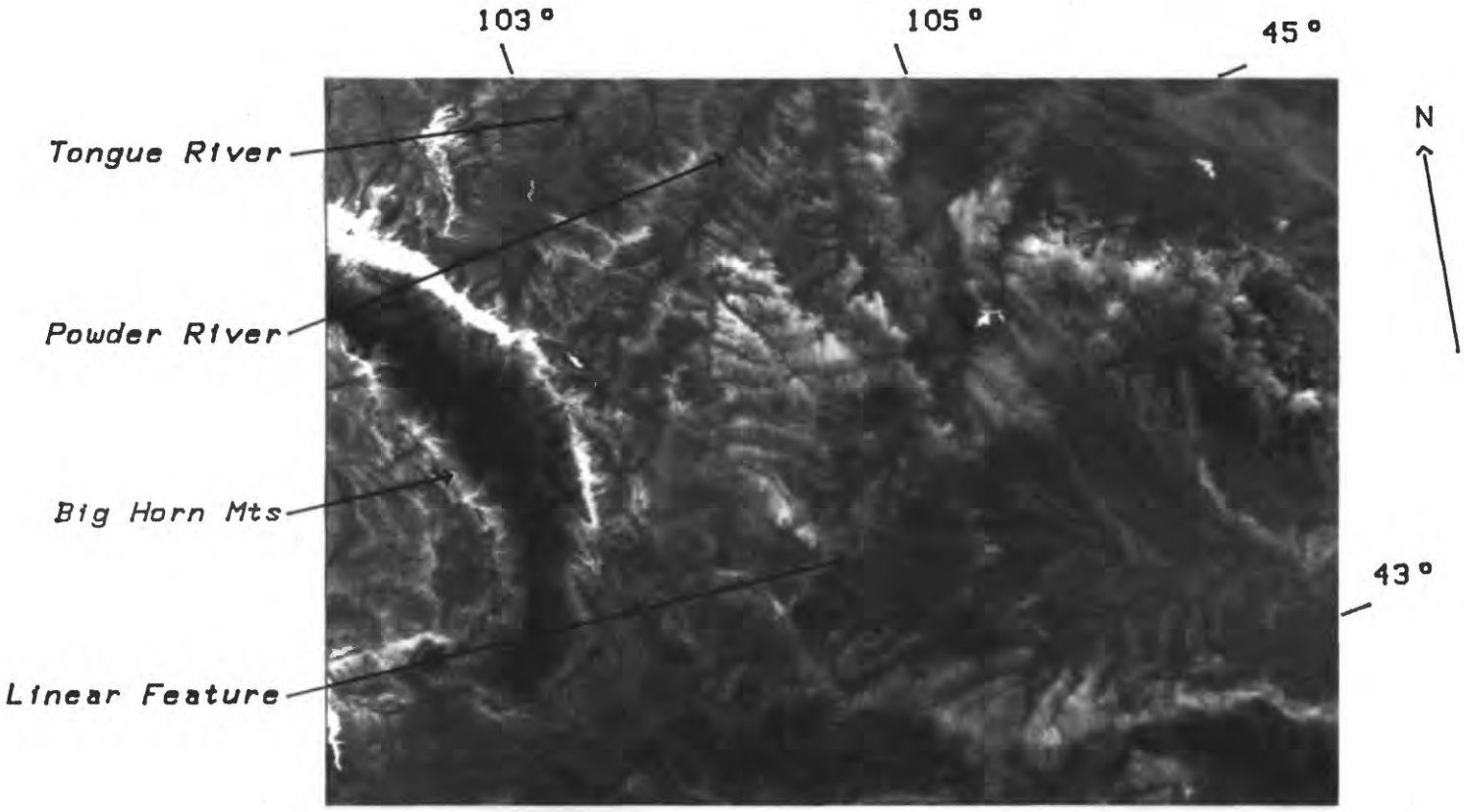

Figure 15.-- Night thermal image, September 27, 1978, of the Powder River Basin, Wyo.

feature on Landsat images (fig. 16a), topographic data (fig. 16b) show this lineament as a subtle drainage divide trending about N55°E. On the thermal images the southward-facing side is cooler by 3° or 4° C, and on the 20 August thermal-inertia image (fig. 7), the south side has a 17 percent lower thermal inertia (1215 TIU) than the north side (1460 TIU). Thus, the feature correlates with a subdued drainage divide but it cannot appear due to the slope effect and must represent - at least in part - a physical property difference across the divide. There is no explanation in existing geologic maps (at scales from 1:24,000 to 1:500,000) for this feature or why it separates temperature and topographic domains. The divide is parallel to the prevailing wind direction from the west-south-west as shown in eolian deposits south of the divide. Moreover, the divide also marks a change in direction of wind deposition; deposits to the north are laid down by winds from the north-northwest. It is possible that the relatively common eolian sand cover south of the divide has controlled drainage habit creating the distinctive topographic texture, and the sandy veneer might possibly cause the domain to have lower thermal inertia due to lower moisture retention. It is not likely, however, that the divide lineament itself is wind related. Extended to the northeast, it continues through the linear gap (of the same strike) between the Black Hills and the Bear Lodge Mountains. More important, it directly overlies one of the most significant breaks (fig. 17) in the aeromagnetic-map pattern (U.S. Dept. of Energy, 1979 a, b, and c) of the whole area, it is parallel to and roughly coincident with an inflection in the ground-water temperatures of the Madison Limestone (fig. 18), and its trend passes through several Tertiary intrusives (fig. 19) and possibly even through Lead, South

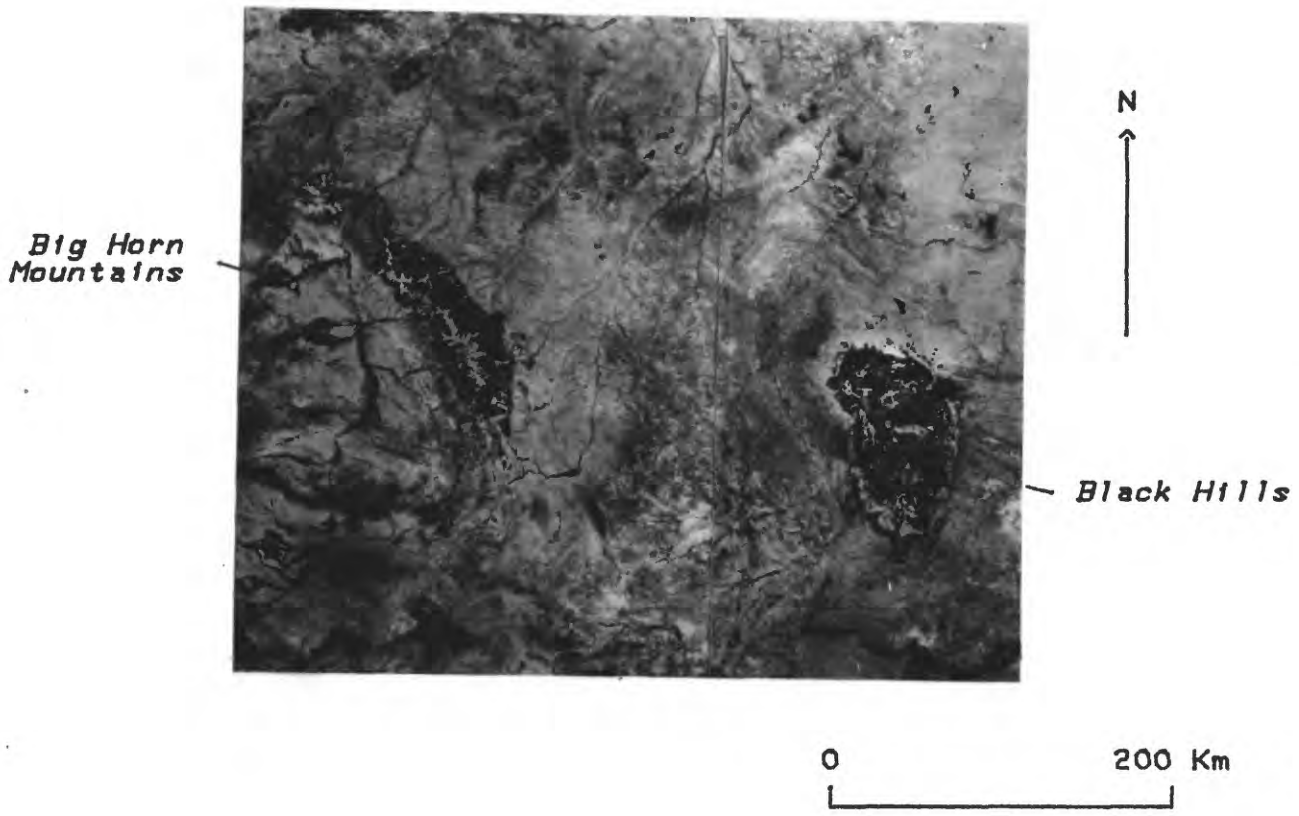

Figure 16a.-- Landsat(Band 5) image of the Powder River Basin Area, Wyo. A north-south mosaic line is present roughly 100 Km west of the Black Hills.

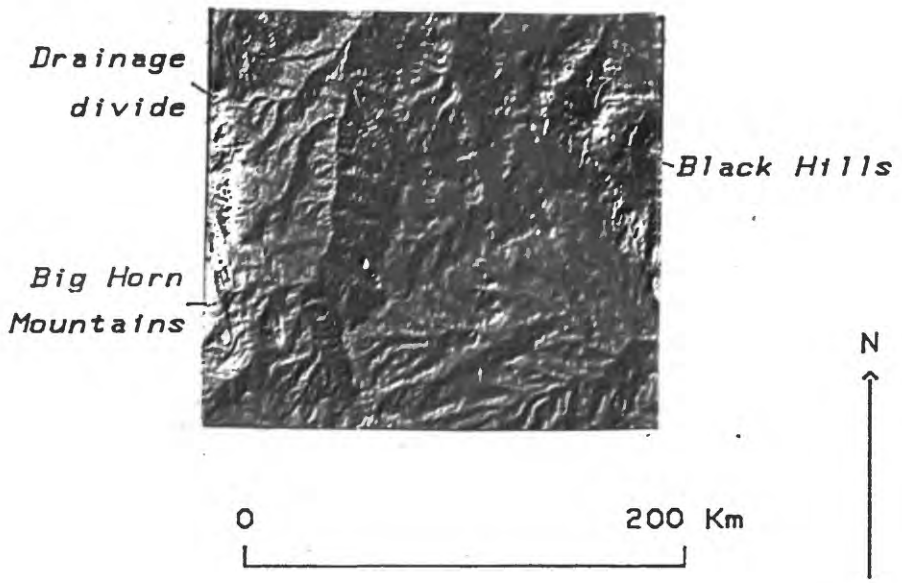

Figure 16b.--Illuminated topography image of the Powder River Basin, Wyo., showing the drainage divide which is coincident with the thermal lineament. The image was computed with a solar declination of -7.8 degrees and a local time of 0930 hrs.

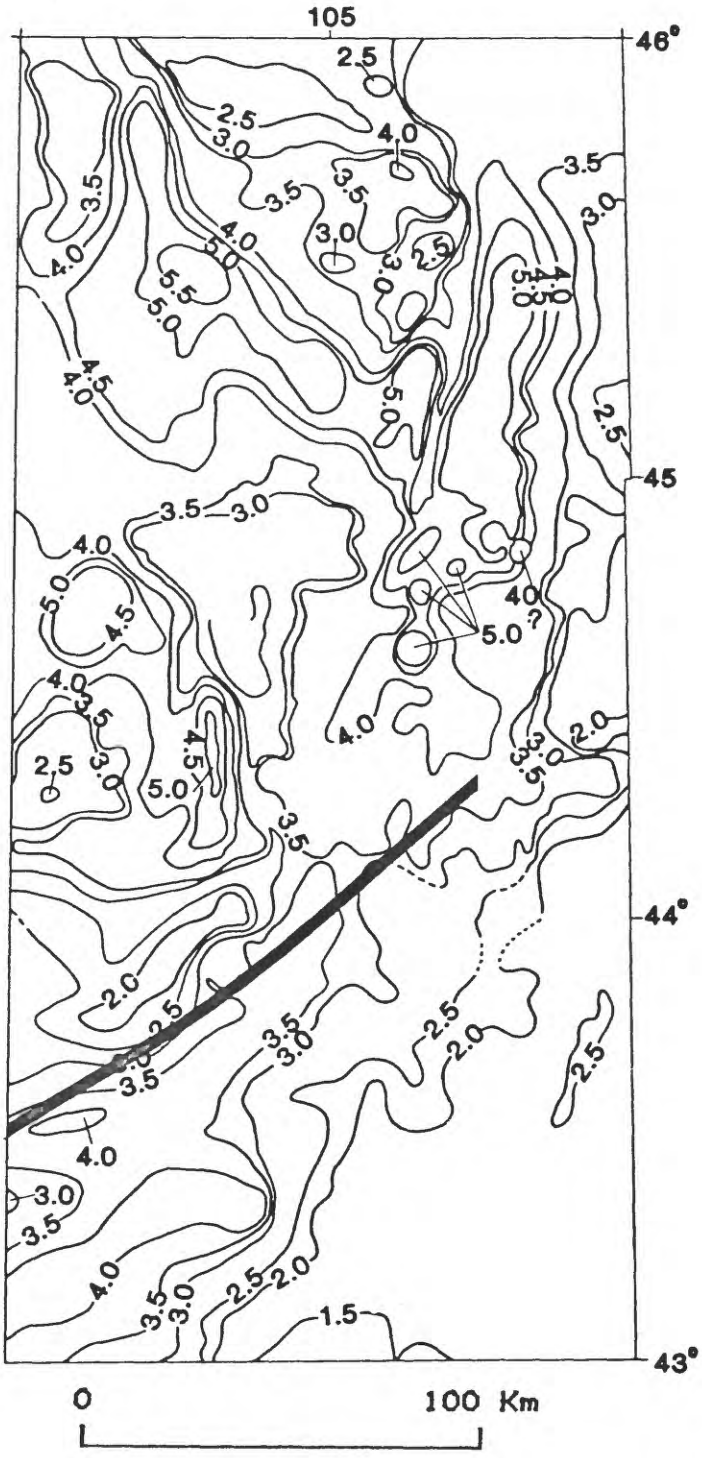

Figure 17.-- Total intensity magnetic field formline map, central Powder River Basin, Wyo.(U.S.Dept of Energy, 1979a-d). The heavy black line shows the position of the thermal lineament.

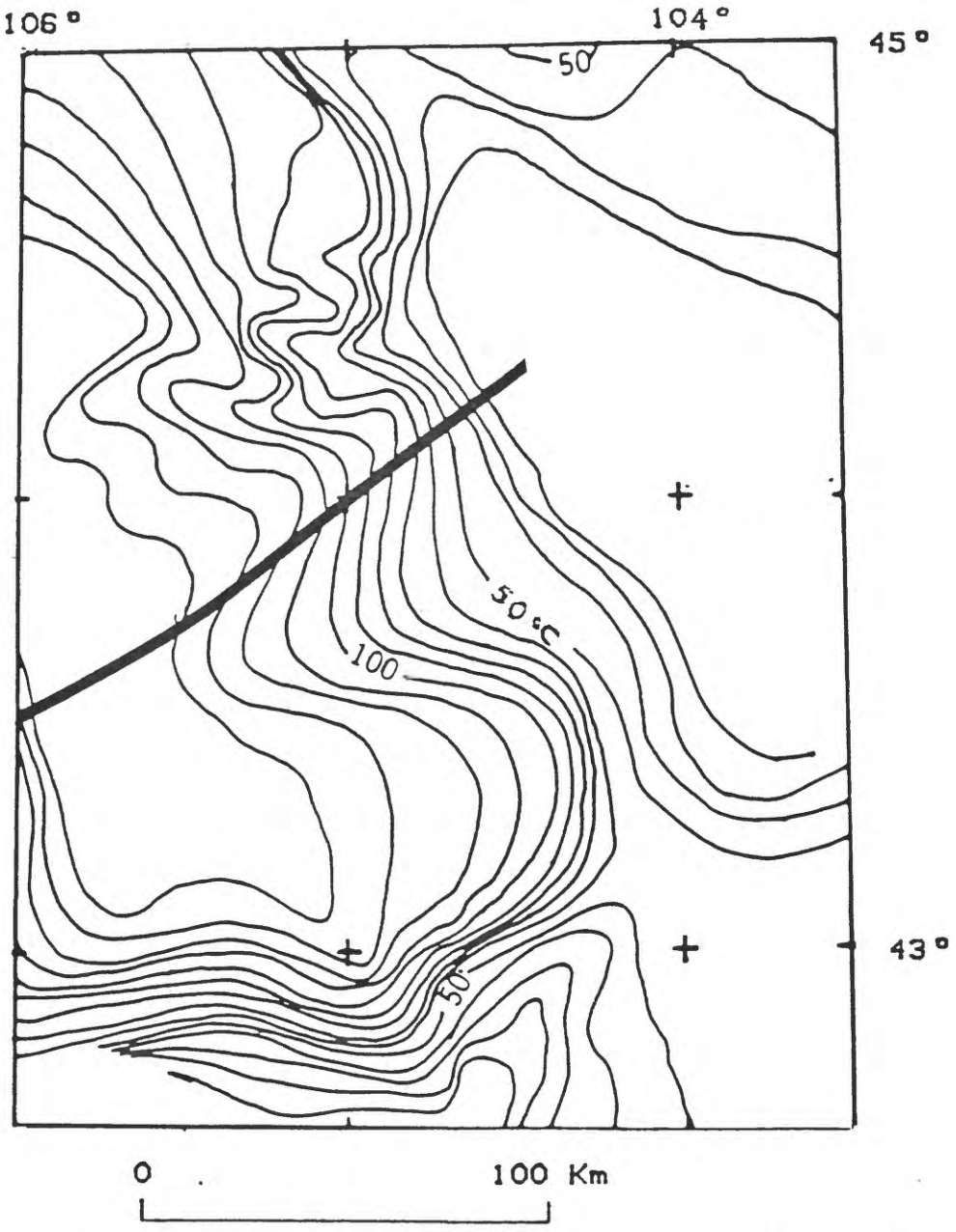

Figure 18.-- Ground water temperatures in the Madison Limestone and equivalent rocks (Head and others, 1978). Heavy black line indicates position of the thermal lineament.

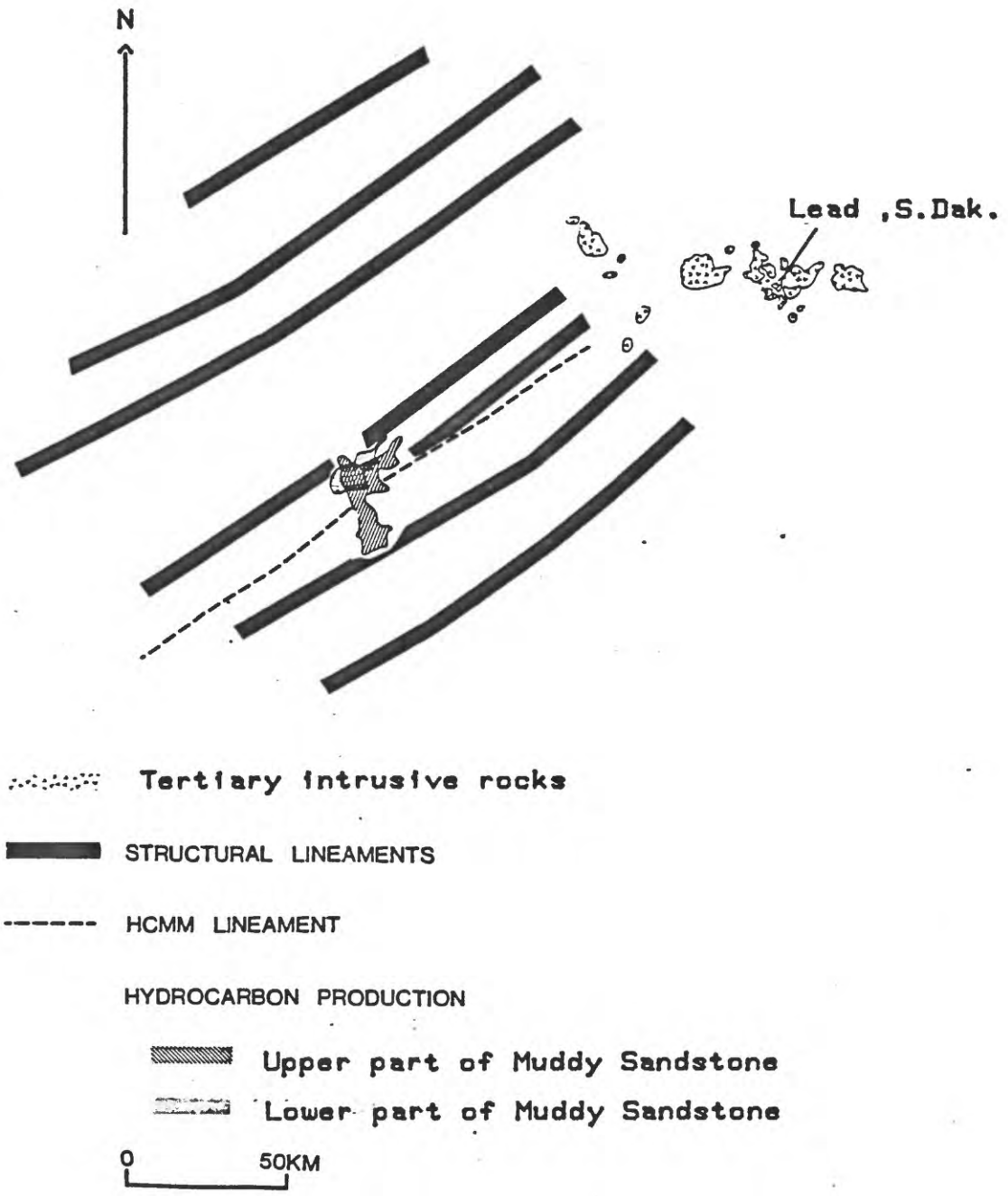

Figure 19.-- Location of the thermal lineament with respect to structural lineaments (Slack,1981) in the Powder River Basin, Wyo.

Dakota location of the Homestake Mine. In addition, stress measurements at Lead (Aggson and Hooker, 1980) imply that the preferred direction for normal faulting would be N50°E, virtually coincident with the orientation of the thermal lineament. Together these pieces of information provide permissive evidence for structural control relating to this feature. A recently published paper (Slack, 1981) presents substantial corroboration for the control. Using subsurface data, Slack proposes that a series of northeast-trending structural lineaments (fig. 19), which he calls the Belle Fourche Arch, have controlled sedimentation in this area and played an important role in determining hydrocarbon accumulation in the southern Powder River Basin. One of his lineaments, Gose Butte, is coincident with part of the thermal feature (fig. 19). Additional supportive evidence for structural control is reflected in the shape of the hydrocarbon producing horizons of the upper and lower parts of the Muddy Sandstone of Cretaceous age (fig. 19).

There is further corroborative satellite evidence for our explanation of the primary cause of the thermal lineament as a thermal-inertia contrast between dissimilar materials. The feature can be seen on two daytime Defense Meteorological Satellite Program (DMSP) thermal satellite images (near noon) and cannot be seen on a nighttime NOAA-5 thermal satellite image (near 9 pm). This latter image is acquired near the time when thermal data should largely be insensitive to thermal-inertia differences because it occurs near the crossing times of the diurnal curves.

We also examined USGS aircraft data across the lineament. Although we had not previously recognized the feature on these data, a very subtle thermal contrast could be observed in the vicinity of the lineament. Largely because

of the slight temperature difference and the regional extent of the feature, it was not recognized on the aircraft data, and this result illustrates convincingly the potential power of regional thermal satellite data over aircraft data for structural-tectonic analysis.

A second, parallel lineament, not a stream divide but separating surface-textural domains, occurs 30 km to the south (figs. 4 and 15) and also overlies an obvious aeromagnetic break. These features appear to mark fundamental structural elements of the southern Powder River Basin and are newly recognized in HCMM data. To the north, parallel lineaments are marked in the images by the Belle Fourche and Little Missouri Rivers.

Information other than on geologic units per se can be gained from these images, most particularly in the demarcation of geomorphic (topographic-temperature) domains and in the discrimination of linear features. Night images are particularly useful in this regard. The 20 August 1978 image (fig. 6) provides very clear definition of major areas of distinctive topography, commonly linked with distinctive temperature patterns. The north and south halves of the basin are distinctly different; the areas east and northeast of the Black Hills differ from each other and from the domains of the basin. Other finer-scale units also are evident. These do not match the mapped geology and, like many geomorphic provinces, are products of a complex development history tied to more factors than the underlying bedrock. We believe that important information can be gained in this aspect of the HCMM images, especially in understanding surface processes during Tertiary and later time. Such information also may lead an understanding of near-surface groundwater hydrology across large, diverse areas. We have examined the domains

from the points of view of mapped geology, ground-water chemistry, mineral and hydrocarbon resources, and tectonic framework, and correspondences are not readily apparent. This is an aspect of the mission data that we did not originally anticipate. However, Schneider and others (1979) showed that the NOAA (National Oceanic and Aeronautics Administration) satellite VHRR (Very High Resolution Radiometer) data with 900-m resolution permitted the defining of geomorphic domains very clearly. This work and our present observations suggest that careful consideration of satellite thermal image data by geomorphologists and hydrologists should be undertaken.

2.3.2 Application to resource studies

2.3.2.1 Oil and gas

It was hypothesized that a few oil and gas fields of the Powder River Basin had enough leakage of gas, probably mostly CO_2, that calcite cementation would have occurred near the surface to make the bedrock more resistant, possibly to form local topographic highs. A few fields do indeed underlie local topographic highs, but this could be fortuitous, and no evidence of leakage and cementation has been cited in the literature. However, a reconnaissance survey of soil-gas helium shows 37 significant helium anomalies within the Wyoming portion of the basin (fig. 20), where most of the oil and gas occurs. The reconnaissance scale of helium sampling does not permit an accurate comparison with individual occurrences of oil and gas except for the largest fields, but it can be said that all but five of the helium anomalies occur over oil and gas fields, and those five are near producing fields. Many

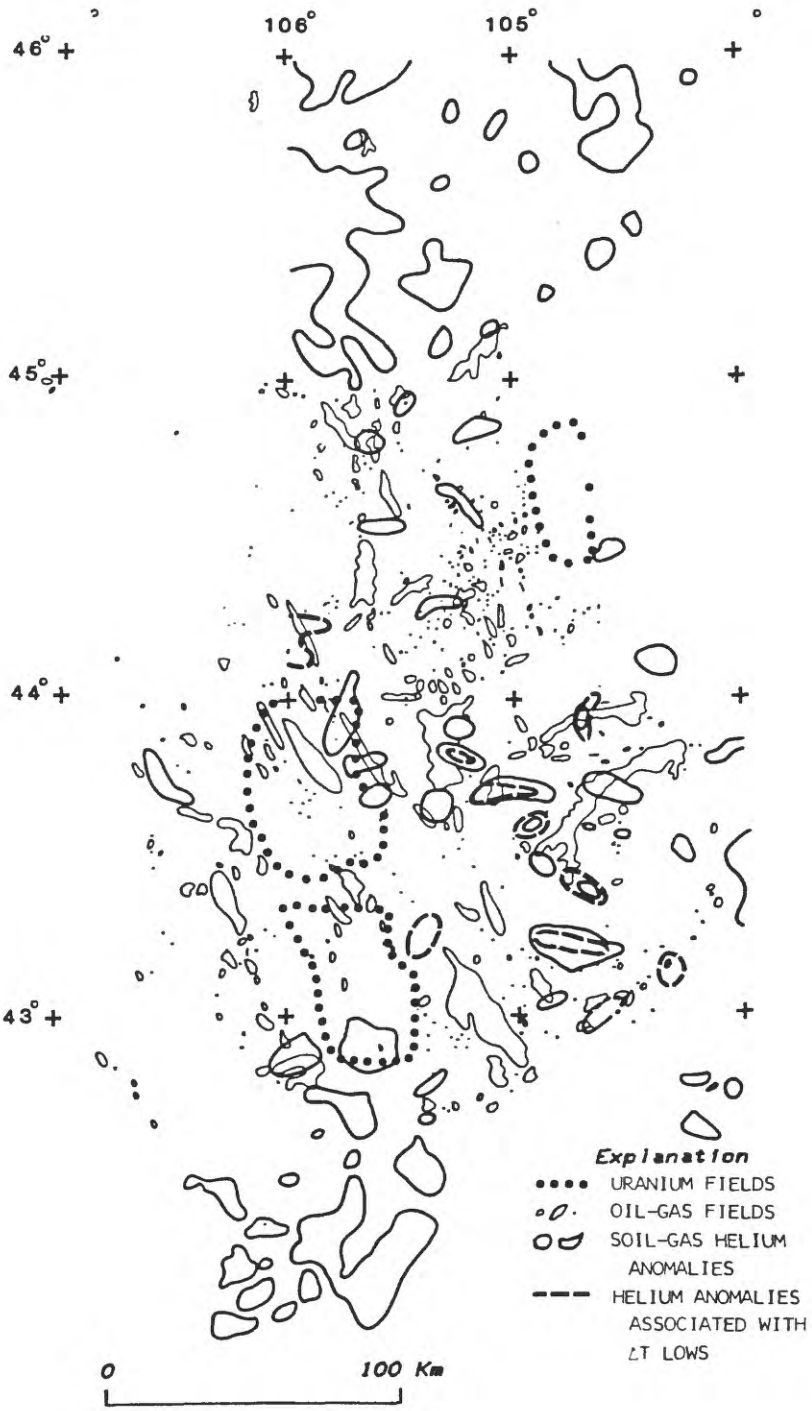

Figure 20.-- Location of helium anomalies, uranium fields, and oil-gas fields in the Powder River Basin, Wyo.

oil and gas fields do not have overlying helium anomalies, and the implication is considered to be that some fields leak gases upward and many more do not. Perhaps 15–20 percent of oil or gas fields might be considered to have leaked helium, although that number might easily prove twice as large if more detailed sampling were done. The percentage of fields where gases may have produced cementation, especially enough to cause detectable changes in surface-temperature character, clearly would be expected to be small. Thus, it is encouraging to note that visual discrimination suggests thermal-inertia anomalies (20 August image, fig. 7) for 9 out of the 37 areas with anomalous helium values (fig. 20). These areas have consistently and noticeably higher values than the surrounding areas, in keeping with expectations if cementation is locally increased. Most of the areas do not have noticeably different topography than their surroundings. Two of the helium-thermal-inertia areas do not overlie known oil or gas fields but both are surrounded by fields and have several dry holes within the areas. The dry holes may have had only subeconomic shows of oil or gas, in which case leakage to the surface may still have occurred; or perhaps holes simply have not been drilled in the right places. The two areally largest helium anomalies, one over a giant gas field and the other in one over the "barren" areas just described, are marked by fairly distinct oval rings in the thermal-inertia pattern.

Helium anomalies are numerous and areally large in the Montana portion of the basin. They occur in a roughly defined ring which corresponds to the perimeter of a roughly circular area of distinctive topography 75 km wide and approximately bisected by the Powder River. This area is virtually without oil-gas production and few wells are shown on available source maps. But the

helium anomalies correspond to the ring of very warm areas seen in the night 20 August image. We know of no reason to expect such helium anomalies in this region except in association with oil and gas, and the warm areas are mostly areas of outcrop, perhaps where cementation is increased. Information has not yet been found on facies in the subsurface rocks that might contain oil and gas. If the facies are not truly favorable, uneconomic amounts of oil and gas might have been present and leakage could have occurred. If the facies are favorable, the area deserves a closer look for exploration.

An additional point of interest is the possible relationship of HCMM lineaments and oil-gas occurrence. The major thermal lineaments transecting the southern part of the basin (fig. 21) define a block that contains most of the significant helium anomalies. Trends in the helium anomalies as contoured from present data commonly parallel HCMM lineaments. The two largest fields, Fiddler Creek and Clareton, are long and narrow and parallel in trend (and between) the basin-transecting thermal lineaments. The west end of the Clareton field ends in a prominent fork, with the southern one of the main lineaments passing through the fork junction.

2.3.2.2 Uranium

The uranium districts of the Powder River Basin (fig. 20) have local areas of surface alteration as large as 5 by 7 km. These, however, are exposed discontinuously, and differ only slightly in lithologic character and thermal properties relative to the surrounding unaltered ground. If the bedrock were totally exposed, an increase in thermal inertia of perhaps 10 percent might make the altered ground detectable. In any case, the only

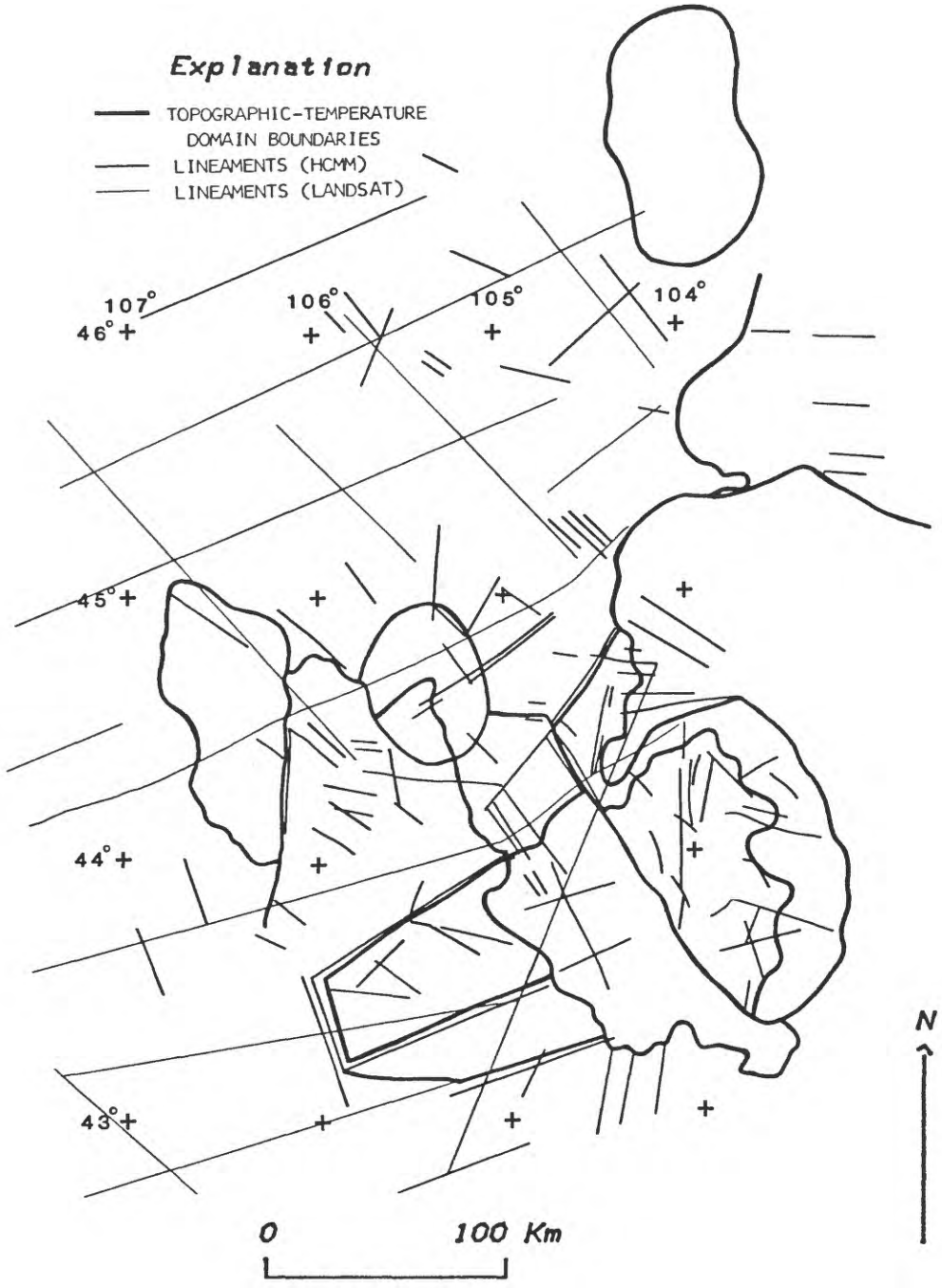

Figure 21.-- Major thermal and Landsat (Marrs and Raines, 1981) lineaments transecting the southern part of the Powder River Basin, Wyo. and boundaries of the topographic-temperature domains.

thermal-inertia data set does not cover the main uranium areas; the 20 August data end east of the districts or have clouds over the fringe areas where uranium ground occurs. We have examined low-altitude aircraft thermal data for the altered ground, and so far "noise" (soil cover, windblown sand, local topography, and moisture variations) seems to completely overwhelm "signal" related to the discrimination problem.

2.3.2.3 Geothermal flux

Another aspect of our study is to examine the utility of HCMM data for geothermal flux mapping. We found that the underground coal fires now burning north of Sheridan, Wyo., are detectable (barely) on nighttime HCMM thermal images. Comparison with a mosaic of aircraft thermal images of this area (fig. 22) illustrates the scale effects on the appearance of small geothermal anomalies. On the aircraft data the anomalies have a sharp, clearly defined pattern, whereas the satellite data show an indistinct pattern which is not distinguishable from geologic and topographic effects. Also, the satellite appearance of drainage features is distinctly different from the aircraft data. From nighttime aircraft data, the Tongue River appears as a sharp warm anomaly with cooler surroundings. The satellite image, because of its coarser resolution, does not discriminate the narrow water channel, and, thus, the drainage appears entirely as a cool zone.

To examine the expression of geothermal anomalies more fully, HCMM scenes of Yellowstone National Park were analyzed. The region has a classic expression of most of the typical hydrothermal features of a vapor-dominated system. A careful comparison between a nighttime image (fig. 23a) and a detailed

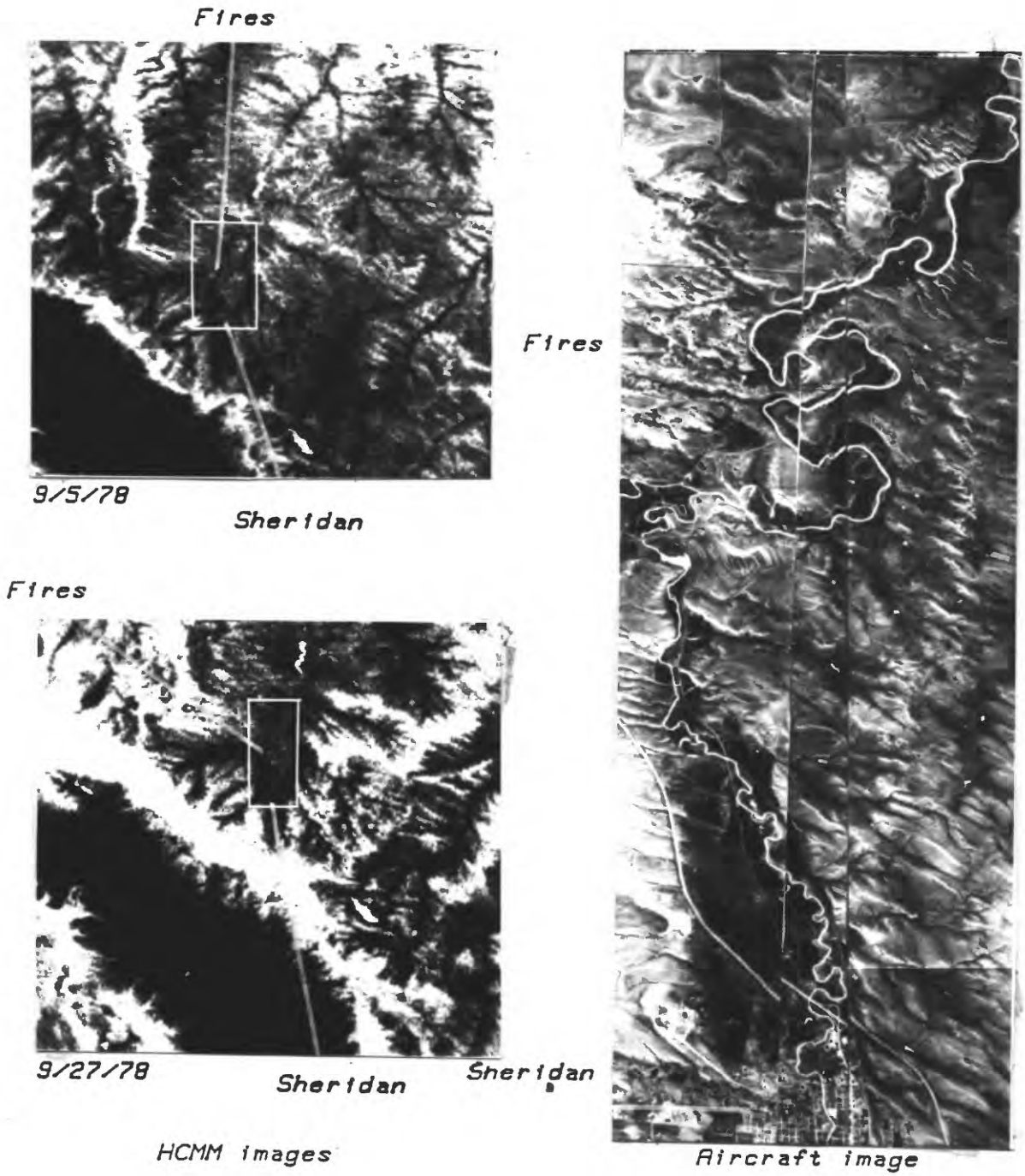

Figure 22.-- Areas of underground coal fires near Sheridan, Wyo., as seen on HCMM and aircraft thermal data.

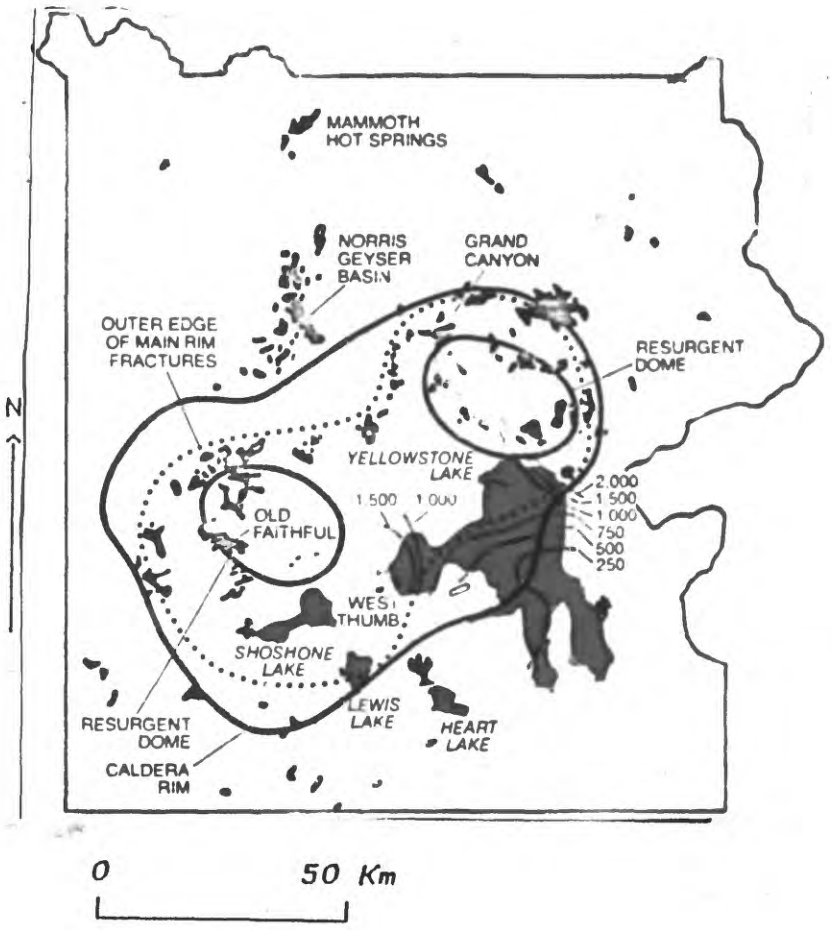

Figure 23a.-- Nighttime thermal image of Yellowstone National Park with caldera outline superimposed.

Figure 23b.-- Location of hydrothermal features (Smith and Christiansen, 1980).

map of the hydrothermal features (Smith and Christiansen, 1980) (fig. 23b) was made using a zoom transfer scope. The hydrothermal features commonly were not expressed as warm anomalies (fig. 24a), and most of the warm anomalies on the images are not hydrothermal-associated features (fig. 24b). These results demonstrate that nighttime satellite images at this scale are unlikely to be useful for detecting similar features elsewhere. Of greater geologic interest was the correlation between the caldera outline, some thermal anomaly lows, and in particular the anomaly bounded by a sharp edge (fig. 23a) which coincides with that part of the gravity field map outlining the southwest side of the caldera (fig. 25b). Although this latter anomaly is a feature with no direct counterpart in Landsat images (fig. 25a), it may provide additional information on the volcanic-tectonic setting. From these brief observations we conclude that the HCMM data can be useful in understanding the regional structural setting of geothermal fields but are not likely to be useful for mapping hydrothermal features.

2.3.2.4 Mapping geologic units in an arid desert environment

The Cabeza Prieta area in Arizona is an arid desert environment with geologic units exposed at a scale suitable for discrimination in HCMM satellite images. The area lies very near the major copper district at Ajo and contains old prospect developments in hydrothermally altered ground. No detailed geologic mapping has been previously done of this area as it contains a proposed Wilderness site. The main objective of our investigation has been to extend the interpretation techniques developed in our Powder River Basin study.

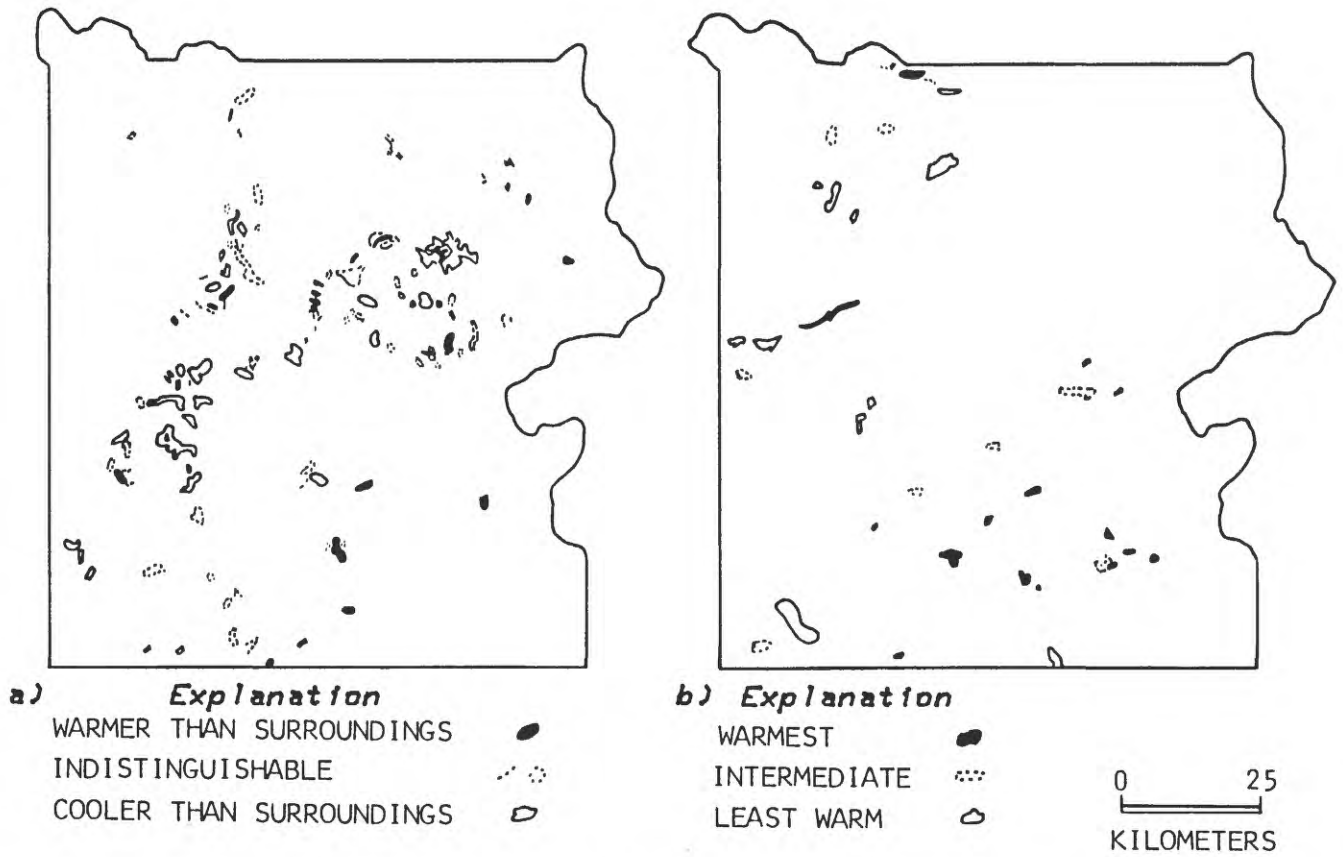

Figure 24a.-- Nighttime temperatures of known hydrothermal features.

Figure 24b.-- Ranking of thermal night anomalies.

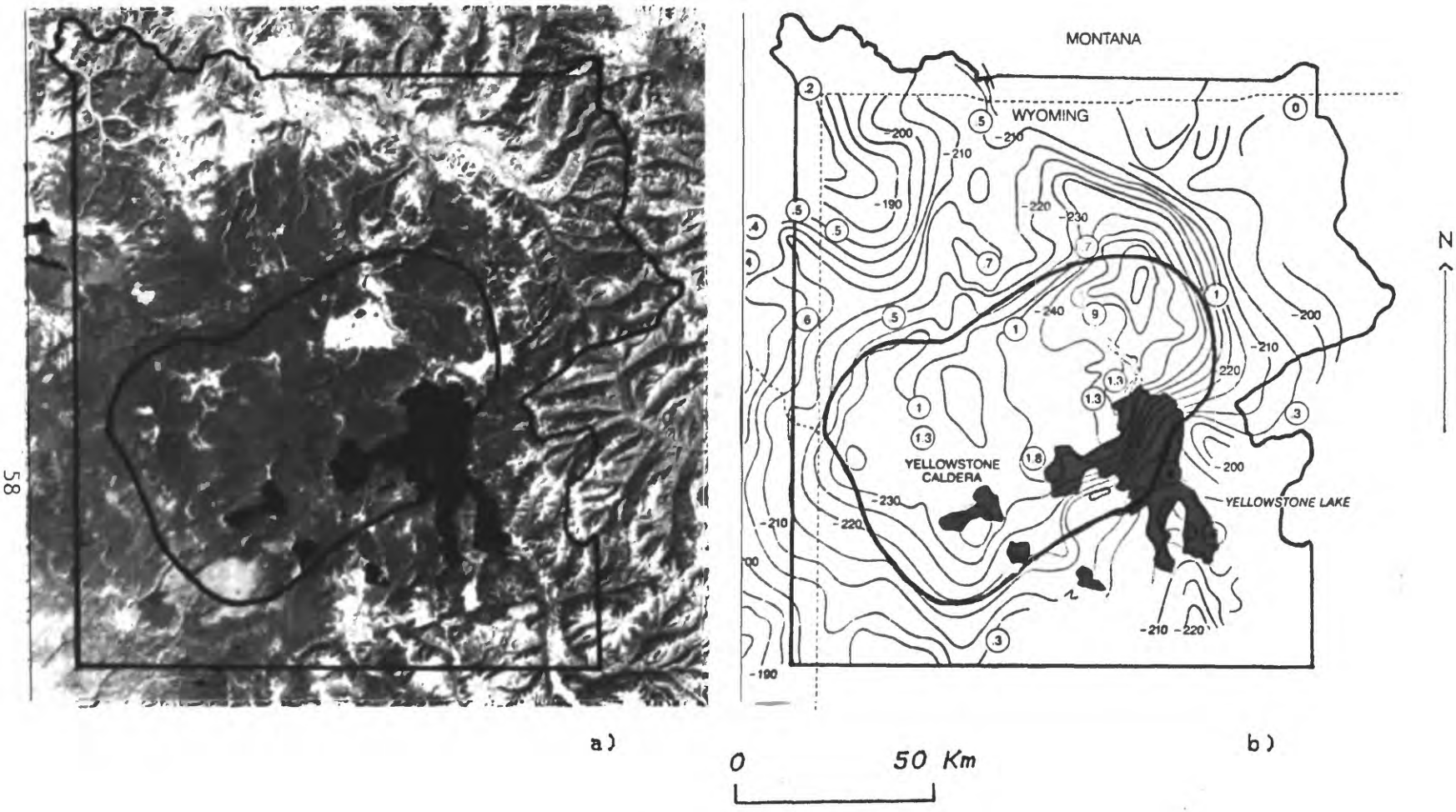

Figure 25a.-- Landsat image of Yellowstone National Park with the caldera and park boundaries outlined.

Figure 25b.-- Gravity field contours (Smith and Christiansen, 1980).

A thermal-inertia image (fig. 26) was constructed using the April 3 and 4, 1979 scenes (AA0342-09150-3; AA0343-20230-1, 2) with 36-h separation between the day and night acquisition times. The image was then compared to the Ajo geologic map (Kahle and others, compilers, 1978) and an estimate was made of the thermal-inertia values of various geologic materials (table 1). Among the sedimentary deposit materials, a wide range of thermal-inertia values was found. From highest to lowest values these included a wet coal-mine dump near Ajo (1890 TIU), active pediment areas (1360 TIU), stablilized dunes (1065-1300 TIU), and active dunes (830-1065 TIU). The most probable explanation for this ranking is due to the strong effect of moisture content on thermal inertia. Generally, active dunes should have the lowest thermal inertia, as observed, owing to their low density and low capacity to retain moisture.

A somewhat surprising result was that the thermal inertias of the various igneous rock units were measurably different, indicating a finer discrimination capability than previous laboratory data in the literature would suggest (Watson, 1979, 1981a). The literature values of thermal-inertias of igneous rocks show no correlation with either composition or grain size and are indistinguishable from each other. In Cabeza Prieta, however, we found that the felsic intrusives (together with gneiss and schist) had the highest thermal inertias (>2200 TIU), that extrusive rocks of mafic composition had intermediate thermal inertias (approximately 2000 TIU) and that extrusive rocks of less mafic composition had the lowest thermal inertia (<1900 TIU). We believe that the felsic intrusives have the highest thermal inertias because of their high quartz content and high surface density and that the differences among extrusive rocks occur because of density differences associated with the amount of

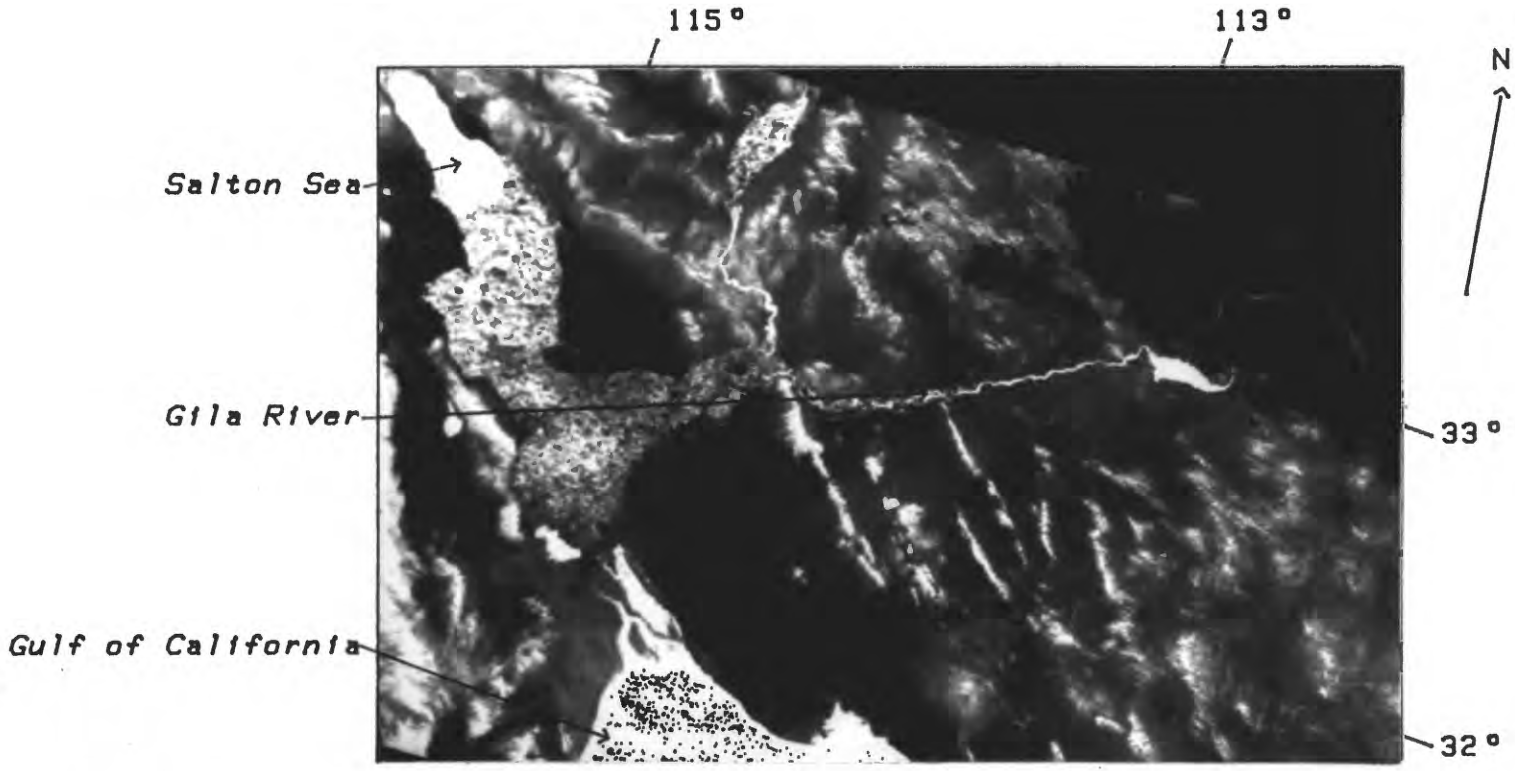

Figure 26.-- Thermal-inertia image, April 3/4, 1979 of Cabeza Prieta, Ariz.

Table 1.--Estimates of thermal inertia of various geologic materials

Geologic Material	Thermal Inertia (TIU)	
	mean	range
Active Dunes	945	(830-1065)
Partially stabilized dunes	1240	
Cluster dunes	1180	(1065-1300)
Active pediment slope	1360	(1300-1475)
Wet mine dump (Ajo)	1890	
Granite, gneiss, schist	2200	(1975-2525)
Mixed intermediate to mafic volcanic rocks	1750	(1550-1950)
Basalt	1950	(1700-2200)

volatiles present during their formation and their mafic content. Although these values are suggestive of the possibility of discriminating among the various units, the large overlap in the range of values (histograms) indicates that classification based solely on thermal inertia differences may not be feasible. The overlap between the units can be attributed to several causes. These units are exposed in the most rugged terrain of the region and thus topographic effects are most pronounced in these parts of the image. The ground that is "sensed" by the technique is a weighted average over the diurnal thermal wavelength (approximately 1 m), with the primary contribution coming from the rock and rock fragments of the upper decimeter. Thus differences in the effects of weathering processes on the various rock types in this environment can produce some degree of thermal-inertia differences.

Because the Powder River Basin was relatively flat terrain the topographic effects were not sufficiently important to be considered. In the Cabeza Prieta area, however, slopes in excess of 20^{o} can be found. To examine the contribution of topography, the thermal inertia measured from remote observations we considered the aspects of elevation and slope separately. The elevation factor due to changes in the solar and sky radiation, has been examined and used to predict the equivalent change in the effective thermal inertia (i.e., that derived from remote rather than in situ measurement) as a function of elevation (Hummer-Miller, 1981b). The effective thermal-inertia gradient under clear-sky conditions should be roughly 100 TIU per kilometer. In Cabeza Prieta, where the maximum relief is 700 m, this maximum correction is only 70 TIU and the factor is additive for increasing elevation (i.e., rocks at higher elevations will appear in the image to have lower thermal inertias).

The slope factor was evaluated by using an algorithm recently developed (Watson, 1981b). The turn has an azimuthal variation proportional to $\cos(\phi - 37.6^{o})$ where ϕ is the direction of slope measured counterclockwise from north, and thus ridges with an axial orientation of roughly N40^{o}W will display a minimal topographic effect. The most consistent topographic grain in the Cabeza Prieta area is northwest-southeast and thus generally satisfies this constraint. The correction can amount to several hundred TIU's for slopes in excess of ten degrees and orientations orthogonal to N40^{o}W (i.e., N50^{o}E).

The primary intent of this study area was to examine correlations between thermal-inertia values and a variety of common rock types exposed in an arid area. In the process of this analysis we also observed, on the night thermal image, a number of linear features associated with known major faults (San Andreas fault, Garlock fault) and the absence of lineaments in an area near Gila Bend which is noted for the absence of structural features (Gila gap). We also were able to determine a measure of the satellite's spatial frequency response (and thus its ability to detect high-contrast linear features) by the observation that Interstate-10 from Gila Bend to Yuma was observable.

3.0 MODEL DEVELOPMENT

Several advances have been made in the development of techniques to analyze thermal-infrared data. An algorithm to determine the sensible-heat flux from simple field measurements (wind speed, air and ground temperatures) has been developed. It provides a direct solution, in parametric form, that can be displayed graphically or tabularly. This method has an advantage over the previous iterative solution in that the computation is both very fast and

it also provides a clearer understanding of the drag coefficient, with its variation and response to different conditions. At low wind speeds the drag coefficient cannot be treated as a constant. Both the computational speed and analysis of the drag coefficient can be important for remote-sensing applications involving thermal scanner data (Watson, 1980).

A substantial advance was the development of a method, based solely on remote-sensing data, to estimate those meteorological effects which must be known for thermal-inertia mapping. It assumes that the atmospheric fluxes are spatially invariant and that the solar, sky, and sensible heat fluxes can be approximated by a simple mathematical form. Coefficients are determined from a least-squares method by fitting observational data to our thermal model. A comparison between field measurements and the model-derived flux shows that good agreement can be achieved. An analysis of the limitations of the method was also made (Watson and Hummer-Miller, 1981a).

This new method of estimating atmospheric parameters was the basis for a revised thermal-inertia algorithm (Watson, 1981a). The new form is:

$$P_{ij} = (\overline{P} \cdot \Delta\overline{V} + C(\lambda,\delta) \quad (\overline{A}-A_{ij}))/\Delta V_{ij}$$

where A_{ij} and ΔV_{ij} are the corresponding albedo and temperature difference of the ith pixel and jth line. $\overline{A}$ and $\overline{V}$ are the mean values for the area in question, and $\overline{P}$ is a select value for the mean thermal inertia (generally 1500 TIU). $C(\lambda,\delta)$ is a function of the site latitude, λ, and the solar declination, δ. The advantage of this algorithm lies in the fact that we are dealing with albedo and thermal differences rather than absolute values. Thus, the computed thermal inertia is less sensitive to offsets caused by calibration

errors or atmospheric backscattering and transmission effects.

Other modeling studies centered around developing an algorithm for elevation correction of temperature and thermal-inertia images (Hummer-Miller, 1981b). They are based on application of the linearized Fourier series method (Watson, 1975; Watson, 1979) to simple forms of the solar flux (Hummer-Miller, 1981a) derived from a representative set of field observations. It was found that flux variations with elevation can cause changes in the mean diurnal temperature gradient from -4^{o} to -14^{o} C per km (evaluated at 2000 m). Changes in the temperature-difference gradient of 1^{o}-2^{o} per km are also produced and these are equivalent to an effective thermal-inertia gradient of 100 TIU per km.

In addition, a simple topographic slope correction method has been developed using the linearized thermal model and assuming slopes less than about 20^{o}. The correction can be used to analyze individual thermal images or composite products such as temperature difference or thermal inertia. Simple curves were determined for latitudes of 30^{o} and 50^{o} (Watson, 1981b). The form is easily adapted for analysis of HCMM images using the DMA (Defense Mapping Agency) digital terrain data (Watson, 1981b).

A major concern in this investigation has been the accurate registration of day and night images. We have developed an image-registration algorithm which appears to be substantially better than the current registration products provided by NASA (Watson and others, 1981). The initial test of this algorithm used the 20 August 1978 data of the Powder River Basin. A small number, less than ten, of very clearly delineated features, generally the water-dam interfaces of reservoirs, were selected as control. Subsequently,

an affine transformation was determined by best fitting these points. Our first test indicates a residual error of < 2 pixels. The NASA product for the same scene displays errors of many pixels resulting in "double drainage" effects and an offset of several kilometers.

During the initial stages of our experimentation with control points, we expected that the drainage pattern in the Powder River Basin was substantial enough to provide extensive control for registration. We discovered, however, that drainages are often unreliable identification features and the resulting control points were too inaccurate to provide the transformation coordinates. We also experimented with cross-correlation techniques in the Cabeza Prieta area but were unsuccessful owing to the strong topographic grain. The affine transformation which we employed has the additional advantage that it can be adapted to very fast computer processing schemes (Braccini and Marino, 1980).

4.0 DIGITAL IMAGE PROCESSING

This section presents an outline of the image processing techniques used in this study. Figure 27 is a simplified flow diagram of the basic processing steps; the computer programs referenced in this diagram are included in Appendix A. The initial processing involves obtaining the HCMM computer-compatible tapes (CCT) and altering the data format to be consistent with our computer software. Sometimes the area of interest spans two scenes and, consequently, must be appended into a single file. To produce enhanced images of these products, the appropriate area of the image is statistically sampled to form a histogram and to derive the mean, median, mode, variance, standard

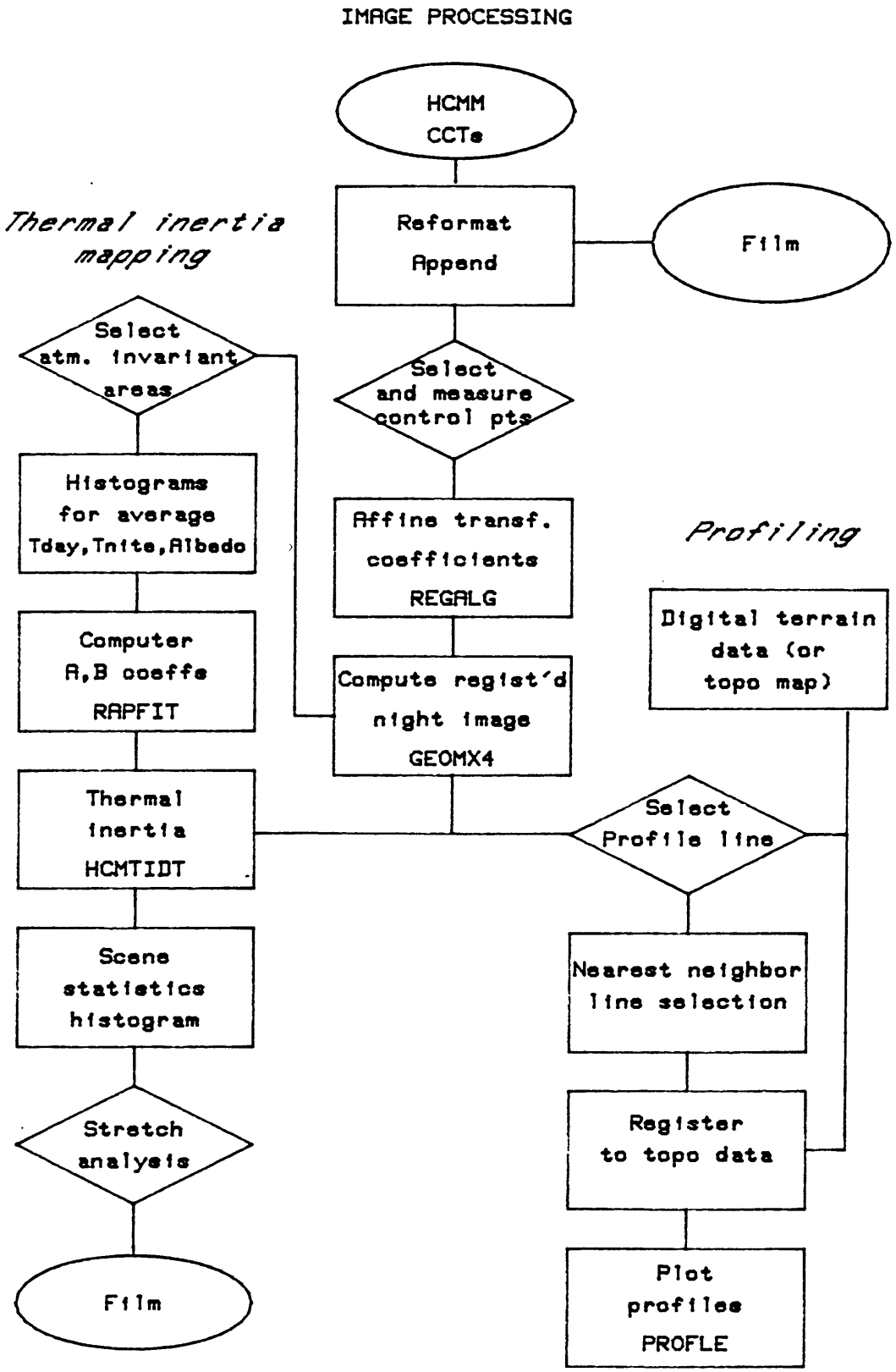

Figure 27.-- Flow chart of the image processing procedure.

deviation, and cumulative frequencies. With these statistics a decision is made as to how the scene contrast should be enhanced using an appropriate transformation of the scene brightness. From our experience a 1 or at most 2 percent linear stretch of the data produces a good starting point. Thus the 1 or 2 percent and 98 or 99 percent points are transformed linearly to the extremes of a 256-step gray scale (0 and 255) and the center density value (Dn) of the distribution is transformed linearly to the center of the gray scale (127 Dn). Other useful products include linear stretches on paper where a single print character is assigned for each Dn value and color-coding on film.

The next processing operation is performed to register the night-thermal file to the day files. This operation, including a discussion of the general considerations, are detailed in Watson and others (1981). Control features are selected from the positive transparency images produced from the CCT and locations are measured to one pixel accuracy. These values are then used to determine the affine coefficients for a best-fit transformation (REGALG). This transformation provides a rotation correction for the inclined satellite orbital tracks, an origin shift, and scale changes both along and across the scan line. The actual registration of the night file is then performed using the affine transformation coefficients in the GEOMX4 computer program. This program assigns radiometric values to the newly registered image employing a nearest-neighbor method.

At this stage the data are in the appropriate format for thermal-inertia and temperature-difference mapping. The algorithms which we use (Watson, 1981a) employ average scene values of albedo, day temperature, and night

temperature. The portion of the scene from which these values are determined is based on the assumption of atmospheric invariance and thus, as a minimum constraint must be cloud-free on both images. The program RAPFIT is then used to compute the appropriate coefficients for this algorithm, and the program HCMTIDT is employed to construct both temperature-difference and thermal inertia files. The resulting files are then processed using these techniques described in the beginning paragraph of 4.0.

Another analysis technique used in this study is to construct profiles across the image data. The end points of particular profiles are chosen and digital values along the line are obtained for all products: day reflectance, day thermal, registered night thermal, and thermal inertia using a nearest-neighbor algorithm. The corresponding elevation profile is obtained by digitizing the appropriate portion of a 1:250,000 topographic map and adjusting it to match the satellite data. This task is made easier if the profiles cross distinct features such as reservoirs and rivers. After the elevation data are registered to the satellite data, the program PROFLE is used to plot the profiles and cross plot pairs of data values. The profiles can be plotted at various scales and thus directly overlaid on any base material for comparison. The cross-plotting option is valuable for examining correlations (for example, we observed that the day thermal versus elevation data fit the adiabatic lapse rate).

5.0 REFERENCES

Aggson, J. R., and Hooker, V. E., 1980, In-situ rock stress determination: techniques and applications, in Underground Mining Handbook: Society of Mining Engineers of AIME, New York, in press.

Braccini, C., and Marino, G., 1980, Fast Geometrical Manipulations of Digital Images: Computer Graphics and Image Processing, v. 13, no. 4, p. 127-141.

Head, W. J., Kilty, K. T., Knotteh, R. K., 1978, Maps showing formation temperatures and configurations of the tops of the Minnelusa Formation and the Madison Limestone, Powder River Basin, Wyoming, Montana, and adjacent areas: U.S. Geological Survey Open-File, 78-905, 10 p.

Hummer-Miller, 1981a, Diurnal variation of four flux parameters fit to field observations: Submitted to Journal of Geophysical Research.

Hummer-Miller, 1981b, Estimation of surface temperature variations due to changes in sky and solar flux with elevation: Geophysical Research Letters (in press).

Kahle, Katherine, Conway, D., and Haxel, G., compilers, 1978, Compilation geologic map of the Ajo 1^{o} by 2^{o} quadrangle, Arizona: Washington D. C., U.S. Geological Survey, 2 sheets, 1:250,000.

Love, J. D., Weitz, J. L., and Hose, R. K., compilers, 1955, Geologic map of Wyoming: Washington, D. C., U.S. Geological Survey, 1 sheet, 1:500,000.

Marrs, R. W., and Raines, G. L., 1981, Tectonics of the Powder River Basin, Wyoming and Montana interpreted from Landsat imagery (abs): Sedimentary Tectonics: Principles and Applications, Laramie, Wyoming, May 3-5, 1981, Summaries, p. 19.

Miller, S. H., Watson, K., and Kipfinger, R., 1980, Ground support data from July 10 to July 29, 1978, for HCMM thermal satellite data of the Powder River Basin, Wyoming: U.S. Geological Survey Open-File, 80-469, 43 p.

Raines, G. L., Offield, T. W., and Santos, E. S., 1978, Remote-sensing and subsurface definition of facies and structure related to uranium deposits, Powder River Basin, Wyoming: Economic Geology, v. 73, p. 1706-1723.

Schneider, S. R., McGinnis, Jr., D. F., and Pritchard, J. A., 1979, Use of satellite infrared data for geomorphology studies: Remote Sensing of Environment, v. 8, p. 313-330.

Slack, P. B., 1981, Paleotectonics and hydrocarbon accumulation, Powder River Basin, Wyoming: American Association of Petroleum Geologists, p. 730-743.

Smith, R. B., and Christiansen, R. L., 1980, Yellowstone Park as a window on the earth's interior: Scientific American, v. 242, p. 104-117.

U.S. Department of Energy, 1979a, Aerial gamma ray and magnetic survey, Powder River II Project, Torrington Quadrangle, Wyoming and Nebraska: Report GJBX-158.

_____1979b, Aerial gamma ray and magnetic survey, Powder River II Project, Gillette Quadrangle, Wyoming: Report GJBX-82.

_____1979c, Aerial gamma ray and magnetic survey, Powder River II Project, Newcastle Quadrangle, Wyoming: Report GJBX-82.

_____1979d, Aerial gamma ray and magnetic survey, Powder River II Project, Ekalaka Quadrangle, Montana: Report GJBX-82.

Watson, K., 1975, Geologic applications of thermal infrared images: Proceedings IEEE, v. 63, p. 128-137.

Watson, K., 1979, Thermal phenomena and energy exchange in the environment, in Mathematical and Physical Principles of Remote Sensing Centre National D'Etudes Spatiales, Toulouse, France, p. 104-174.

_____1980, Direct computation of the sensible heat flux: Geophysical Research Letters, v. 7, no. 8, p. 616-618.

_____1981a, Regional thermal-inertia mapping from an experimental satellite: Geophysics (in press).

_____1981b, Topographic slope correction for analysis of thermal-infrared images: NTIS (in press).

Watson, K., and Hummer-Miller, S., 1981a, A simple algorithm to estimate the effective regional atmospheric parameters for thermal-inertia mapping: Remote Sensing of the Environment (in press).

Watson, K., Hummer-Miller, S., and Sawatzky, D. L., 1981b, Registration of Heat Capacity Mapping Mission day and night images: Photogrammetric Engineering (in press).